Accepted to the Astrophysical Journal: Oct 12, 2001
Preprint typeset using LATEX style emulateapj v. 20/04/00

THE UCSD HIRES/KECKI DAMPED Lyα ABUNDANCE DATABASE[1] II. THE IMPLICATIONS

JASON X. PROCHASKA[2,3]
The Observatories of the Carnegie Institute of Washington
813 Santa Barbara St.; Pasadena, CA 91101

AND

ARTHUR M. WOLFE[2]
Department of Physics, and Center for Astrophysics and Space Sciences
University of California, San Diego; C–0424; La Jolla; CA 92093
Accepted to the Astrophysical Journal: Oct 12, 2001

ABSTRACT

We present a comprehensive analysis of the damped Lyα abundance database presented in the first paper of this series. This database provides a homogeneous set of abundance measurements for many elements including Si, Cr, Ni, Zn, Fe, Al, S, Co, O, and Ar from 38 damped Lyα systems with $z_{abs} > 1.5$. With little exception, these damped Lyα systems exhibit very similar relative abundances. There is no significant correlation in X/Fe with [Fe/H] metallicity and the dispersion in X/Fe is small at all metallicity.

We search the database for trends indicative of dust depletion and in a few cases find strong evidence. Specifically, we identify a correlation between [Si/Ti] and [Zn/Fe] which is unambiguous evidence for depletion. Following Hou et al. (2001), we present [X/Si] abundances against [Si/H] $+ \log N$(HI) and note trends of decreasing X/Si with increasing [Si/H] $+ \log N$(HI) which argue for dust depletion. Similarly, comparisons of [Si/Fe] and [Si/Cr] against [Si/H] indicate significant depletion at [Si/H] > -1 but suggest essentially dust-free damped systems at [Si/H] < -1.5 dex.

We present a discussion on the nucleosynthetic history of the damped Lyα systems by focusing on abundance patterns which are minimally affected by dust depletion. We find [Si/Fe] $\to +0.25$ dex as [Zn/Fe] $\to 0$ and that the [Si/Fe] values exhibit a plateau of $\approx +0.3$ dex at [Si/H] < -1.5 dex. Together these trends indicate significant α-enrichment in the damped Lyα systems at low metallicity, an interpretation further supported by the observed O/Fe, S/Fe and Ar/Fe ratios. Comparing the relative abundances of the Fe-peak elements, we identify important offsets from solar relative abundances for Cr, Ni, and Fe which suggest variations in nucleosynthesis along the Fe-peak. Finally, the damped Lyα systems exhibit a modest odd-even effect revealed by Si/Al, [Si/Al] $\approx +0.4$ dex, which is significantly smaller than values observed in Galactic halo stars of comparable metallicity. These observations present strong evidence that the damped Lyα systems and Galactic halo had different enrichment histories.

To assess the impact of dust obscuration, we present estimates of the dust-to-gas ratios for the damped Lyα sightlines and crudely calculate dust extinction corrections. The distribution of extinction corrections suggests the effects of dust obscuration are minimal and that the population of 'missing' damped systems has physical characteristics similar to the observed sample.

We update our investigation on the chemical evolution of the early universe in neutral gas. The results are in good agreement with our previous work, but we emphasize two differences: (1) the unweighted and N(HI)-weighted [Fe/H] mean metallicities now have similar values at all epochs except $z > 3.5$ where small number statistics dominate the N(HI)-weighted mean; (2) there is no evolution in the mean [Fe/H] metallicity from $z = 1.7 \to 3.5$ but possibly a marked drop at higher redshift.

We conclude with a general discussion on the physical nature of the damped Lyα systems. We stress the uniformity of the damped Lyα chemical abundances which indicates that the protogalaxies identified with damped Lyα systems have very similar enrichment histories, i.e. a nearly constant relative contribution from Type Ia and Type II SN. The damped Lyα systems also show constant relative abundances within a given system which places strict constraints on the mixing timescales of the damped systems and may pose a great challenge to the protogalactic clump scenarios favored by hierarchical galaxy formation.

Subject headings: galaxies: abundances — galaxies: chemical evolution — quasars : absorption lines — nucleosynthesis

1. INTRODUCTION

Astronomers have long used high resolution spectroscopy to examine the chemical abundances of stars in the Milky Way. Besides meteoritic sampling, these studies provide the most accurate assessment of absolute and relative nucleosynthetic yields in our Galaxy. In turn, the results test existing theories of nucleosynthesis as well as inspire new processes (e.g. Wheeler et al. 1989; Edvardsson et al. 1993; McWilliam et al. 1995). A principal goal of modern efforts is to extend these studies to the most extreme metal-poor stars whose enrichment might arise from a few or even a single supernova. Similar chemical abundance studies have been pursued within the Galaxy's interstellar medium (ISM). Spurred by Lyman Spitzer's inspiration, UV spectroscopy acquired from space telescopes has led to a detailed examination of the chemical and physical properties of this gas. Many of the same elements studied in stars are analyzed in the ISM, but in contrast, the ISM abundance patterns reflect more on processes of dust formation and destruction than nucleosynthesis (e.g. Spitzer and Fitzpatrick 1993; Savage & Sembach 1996).

With the advent of 10m class telescopes, scientists now perform ISM observations of high z galaxies in a manner analogous to studies of the Milky Way ISM, i.e., through an analysis of high resolution spectroscopy of distant quasars whose sightlines penetrate protogalaxies (e.g. Wolfe et al. 1994; Prochaska & Wolfe 1996, hereafter PW96; Lu et al. 1996, hereafter L96; Prochaska & Wolfe 1999, hereafter PW99; Pettini et al. 2000). The majority of these quasar absorption line (QAL) studies have focused on the chemical abundances of the damped Lyα systems: neutral hydrogen gas layers with HI column density, $N(\mathrm{HI}) \geq 2 \times 10^{20}\,\mathrm{cm}^{-2}$. These QAL systems are the dominant reservoir of neutral baryons at every observable epoch and are routinely identified as the progenitors of modern galaxies. Indeed, this was the founding principle of the first damped Lyα surveys (Wolfe et al. 1986) and is well supported by the correspondence of the inferred baryonic mass density of damped systems at $z \sim 2$ and the mass density in stars today (Lanzetta et al. 1995; Wolfe et al. 1995; Storrie-Lombardi and Wolfe 2000).

One of the most exciting aspects of the damped Lyα systems is the fact that they provide a means for assessing the chemical abundances of many elements for galactic systems in the early stages of evolution. High resolution studies of metal-poor stars may offer a complementary view, but at present these studies are limited to the Milky Way and a few other nearby systems. Therefore, interpretations associated with metal-poor stars are strictly limited by the fact that one is not sensitive *a priori* to a wide range of star formation histories; there is always the possibility that the Milky Way represents a unique path in the nucleosynthetic history of the universe. In contrast, the damped Lyα systems presumably probe protogalaxies with a range of characteristics (e.g. mass, morphology, age). At some level, this diversity is a hindrance because our very limited knowledge of these properties. Nevertheless, the damped Lyα systems provide a valuable laboratory for research on stellar nucleosynthesis.

Because the damped Lyα systems exhibit sub-solar metallicities, including several with [Fe/H] < -2, one expects their observed abundance patterns to arise from a non-solar nucleosynthetic pattern modified by the depletion of refractory elements onto dust grains. Ideally, one aims to disentangle the two patterns in order to gauge the implications of dust depletion (e.g. obscuration bias; Fall & Pei 1993) and reveal the chemical enrichment history of these first galaxies. Unfortunately, the analysis is confused by the limited number of routinely observed elements (Fe, Si, Cr, Ni, Al, Zn) and the coincidence between a standard Type II SN pattern and the warm halo ISM dust depletion pattern (L96; PW99; Prochaska et al. 2000, hereafter P00). The challenge is to identify abundance ratios which lift this degeneracy.

In this paper we analyze recently published chemical abundances of a large database of $z > 1.5$ damped Lyα systems (Prochaska et al. 2001, Paper I). All of the data were obtained with the HIRES spectrograph (Vogt et al. 1994) on the Keck I telescope, were reduced with the MAKEE software package, and analyzed with the same techniques (see Paper I for complete details). It is a large homogeneous dataset, ideal for comprehensive analysis. In the following, we restrict ourselves to five main areas: (§ 2) an element by element discussion of abundance trends with Fe metallicity; (§ 3) an investigation of dust depletion; (§ 4) implications for nucleosynthesis in these protogalaxies; (§ 5) evidence for/against dust obscuration; and (§ 6) the chemical enrichment history inferred from damped Lyα systems. We conclude (§ 7) with a general discussion of the damped Lyα systems including speculations on their physical nature. Given the length of this manuscript, we encourage the reader to focus on areas of primary interest and refer to the summary tables throughout.

2. ELEMENTAL ABUNDANCES

In this section we present the most important elemental abundances for our sample of damped Lyα systems, stressing the new results from this paper. Throughout the analysis we adopt no ionization corrections, i.e., we assume that the column density of element X is equal to the column density of the dominant ionization state in neutral hydrogen gas: Fe+ for Fe, O^0 for O, H^0 for H. This assumption is theoretically motivated (e.g. PW96; Viegas 1994), but not well established empirically. Recent calculations indicate ionization corrections should be small for the majority of elements considered here (Vladilo et al. 2001), but future damped Lyα studies need to address this point unambiguously (Prochaska, Howk, O'Meara, & Tytler 2002).

Following standard practice in stellar abundance studies, we plot the abundance of each element with respect to Fe relative to the solar ratio, $[\mathrm{X/Fe}] \equiv \log[N(\mathrm{X})/N(\mathrm{Fe})] - \log[N(\mathrm{X})/N(\mathrm{Fe})]_\odot$, against [Fe/H]. In a stellar analysis, this comparison highlights trends which reflect nucleosynthetic processes convolved with the star formation history. For the damped Lyα systems, the analysis is sensitive to the combined effects of nucleosynthesis and dust depletion.

[1]http://kingpin.ucsd.edu/~hiresdla

[2]Visiting Astronomer, W.M. Keck Telescope. The Keck Observatory is a joint facility of the University of California and the California Institute of Technology.

[3]Hubble Fellow

Unless otherwise noted, we plot 1σ error bars[4] derived from the apparent optical depth method (AODM; Savage and Sembach 1991) as listed in Paper I. For each element, we consider several simple statistics (e.g. a Pearson's test to investigate linear correlations) of the observed sample excluding all upper and lower limits. A summary of this section is given in Tables 2 and 3 (§ 2.4).

2.1. *Fe-Peak Elements – Cr, Mn, Co, Fe, Ni, Zn*

We begin with the elements whose atomic numbers are near Fe, the so-called Fe-peak elements. We include Zn, although it is not a true Fe-peak element and is probably produced through different nucleosynthetic processes (Hoffman et al. 1996; Umeda & Nomoto 2001).

2.1.1. *Iron*

Almost all of our interpretations of dust depletion, dust obscuration, and nucleosynthesis are drawn in part from Fe measurements and, therefore, it is important to highlight the uncertainties associated with measuring N(Fe). The most significant uncertainties at the time of this publication are in the oscillator strengths of the Fe II $\lambda\lambda$1608,1611 transitions. For Fe II 1608, the f-value is taken from Bergeson et al. (1996) who attribute a 9% error to their laboratory value which translates to ≈ 0.035 dex uncertainty. For Fe II 1611, we consider the most reliable value to be the theoretical value from Raassen & Uylings (1998). Until now, most damped Lyα analyses have relied upon the f_{1611} value presented by Cardelli & Savage (1995) from their empirical analysis of several Fe II transitions observed in the ISM. The difference is significant; the Raassen & Uylings (1998) f-value implies an ≈ 0.1 dex lower $N(\mathrm{Fe}^+)$ value than the Cardelli & Savage (1995) value. As discussed in Paper I, the $N(\mathrm{Fe}^+)$ value derived from Fe II 1611 is in good agreement with the values from Fe II 2249 and 2260 in the systems where we observed all three profiles. Therefore, we are reasonably confident in the adopted Fe II 1611 oscillator strength.

For some of the following analysis, we adopt a proxy for Fe (e.g. Cr, Ni, Al) when we have no reliable $N(\mathrm{Fe}^+)$ measurement. In these cases, we assume [Fe/H] = [Ni/H] − 0.1, [Fe/H] = [Cr/H] − 0.2, or [Fe/H] = [Al/H] for reasons which will become obvious below. When we have made this substitution, we plot these specific data points with a unique symbol and generally do not include their values in any statistical analysis (i.e. means, medians, Pearsons' tests).

2.1.2. *Chromium*

Figure 1 presents the [Cr/Fe] values vs. [Fe/H] for our complete sample. Nearly every damped system shows an enhanced Cr/Fe ratio, a behavior first noted in L96 and emphasized in PW99. The median enhancement is +0.17 dex which is suggestive of dust depletion because no stellar population shows enhanced Cr/Fe whereas dust depleted ISM sightlines do exhibit a mild Cr overabundance. One also notes a slight anti-correlation between [Cr/Fe] and metallicity. If the trend is not the result of small number statistics, it may have significant implications for dust depletion (§ 3.1).

[4]Note the error adopted is the quadrature sum of the errors in logarithmic space

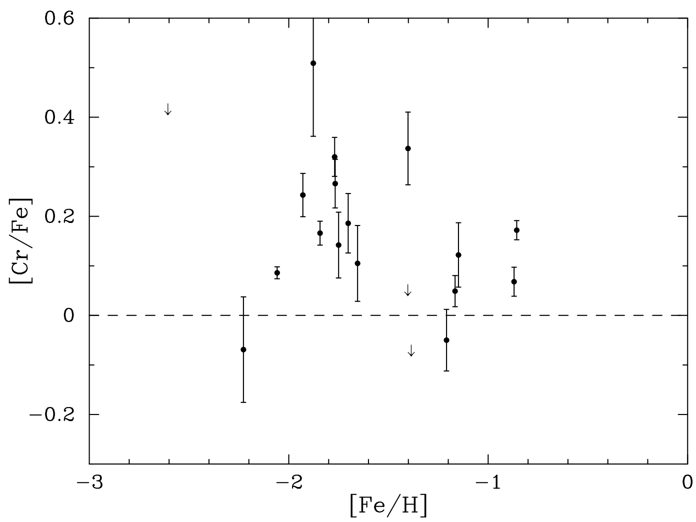

FIG. 1.— [Cr/Fe] abundance ratios vs. [Fe/H] metallicity for our complete sample of damped Lyα systems. Nearly every system shows a mild enhancement and there is a mild trend of decreasing Cr/Fe with increasing metallicity (although $P_{Pears} = 0.52$ due to the system at [Fe/H] = −2.2). The dashed line at [Cr/Fe] = 0 indicates the solar meteoritic Cr/Fe ratio.

2.1.3. *Cobalt*

Ellison, Ryan, & Prochaska (2001) recently drew attention to the prospect of measuring Co in the damped Lyα systems. Figure 2 plots the [Co/Fe] values for our full sample, with all but one measurement an upper limit on $N(\mathrm{Co}^+)$. We report a measurement for the system at $z_{abs} = 1.920$ toward Q2206–19 which is consistent with the value reported by Ellison, Ryan, & Prochaska (2001).

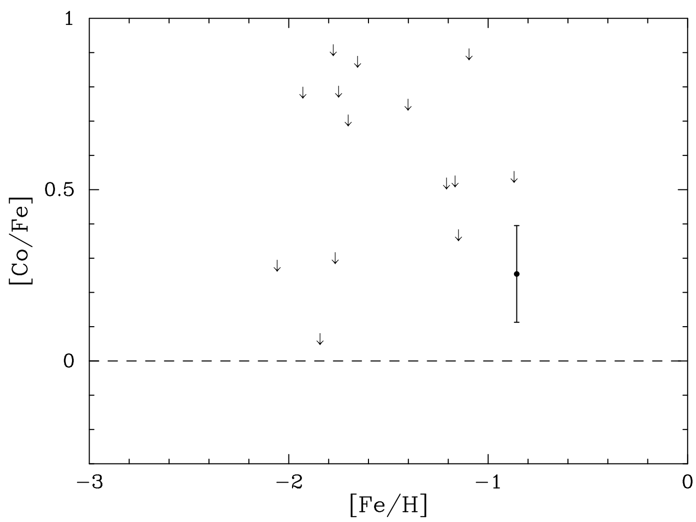

FIG. 2.— [Co/Fe] abundance ratios vs. [Fe/H] metallicity for our complete sample of damped Lyα systems. We report only a single detection and are even suspect of its value. With improved S/N, several of these systems might present meaningful constraints on Co/Fe. The dashed line at [Co/Fe] = 0 indicates the solar meteoritic Co/Fe ratio.

Our value is based on the very weak Co II 1574 transition, however, and is therefore highly suspect. Furthermore, the upper limits that we place on $N(\mathrm{Co}^+)$ from Co II 1941 and 2012 are smaller than the value for Co II 1574 and also are in conflict with the value implied by Ellison et al. It is possible that the differences are due to continuum error, although we suggest Ellison et al. slightly overestimated $N(\mathrm{Co}^+)$.

The effect of dust depletion on the Co/Fe ratio is not well understood, in particular because Co^+ has been very rarely detected in the ISM. From the measurements for ζ Oph, it appears that Co has a refractory nature similar to Fe and the other Fe-peak elements. This is expected given the correlation observed between the gas-phase abundance and condensation temperature of many elements (e.g. Jenkins 1987). Therefore, a significant departure from the solar ratio might indicate important nucleosynthetic processes (e.g. McWilliam 1997). Figure 2 indicates several upper limits whose value approach the solar abundance. Greater attention should be given to these few systems where improved S/N can provide meaningful Co measurements.

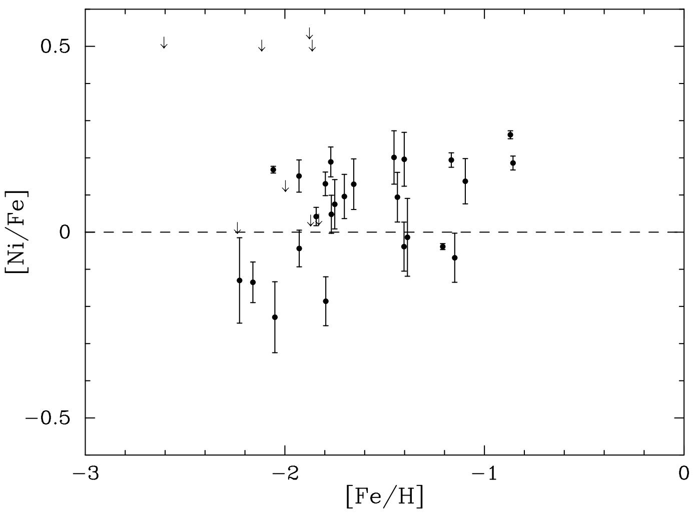

FIG. 3.— [Ni/Fe] abundance ratios vs. [Fe/H] metallicity for our complete sample of damped Lyα systems. The values scatter about the solar ratio with the majority exhibiting a small enhancement. We also note a significant trend with metallicity ($P_{Pears} = 0.02$). The dashed line at [Ni/Fe] = 0 indicates the solar meteoritic Ni/Fe ratio.

2.1.4. *Nickel*

Figure 3 plots [Ni/Fe] vs. [Fe/H] for 31 of our damped Lyα systems. Although the [Ni/Fe] points scatter about the solar value, the majority are mildly enhanced. The unweighted mean of all measurements (no limits) is $<$ [Ni/Fe] $>= +0.07 \pm 0.03$ and the median value is +0.095. This enhancement is not observed in the ISM and conflicts with empirical trends in metal-poor stars although a Ni/Fe enhancement is predicted in core-collapse explosions of massive Pop III stars (Umeda & Nomoto 2001). Of course, a small error may exist in the Ni^+ or Fe^+ atomic data implying this mild enhancement. An enhanced Ni/Fe ratio can also arise from photoionization (Howk & Sembach 1999), but one would also predict a large Ni/Cr ratio where the opposite is observed. Finally, it is possible the enhanced Ni/Fe values reflect intrinsic differences in abundance patterns between stellar atmospheres and the damped Lyα systems.

2.1.5. *Zinc*

Zinc plays a pivotal role in interpreting the abundance patterns of the damped Lyα systems. Since Pettini et al. (1994) demonstrated that most damped systems exhibit enhanced Zn/Cr ratios, the community has generally accepted the notion that the refractory elements (e.g. Fe, Ni, Cr) are mildly depleted. Because of the impact of this element, it is important to carefully examine any issues which influence measurements of $N(\mathrm{Zn}^+)$.

While there are two strong Zn II transitions at 2026Å and 2062Å, the latter transition is often blended with the Cr II 2062 transition. Therefore we rely primarily on the Zn II 2026 profile, in particular because the AODM does not easily account for line blending. The difficulty, however, is that the Zn II 2026 profile may also be blended with two other transitions: Mg I 2026 and Cr II 2026 with separations from Zn II 2026 of +52 km/s and +20 km/s respectively. Luckily, the oscillator strength of the Cr II 2026 transition is small enough that it should not significantly affect the $N(\mathrm{Zn}^+)$ measurement. The Mg I 2026 profile, meanwhile, has been considered in previous works (e.g. Pettini et al. 1994), but was generally ignored in PW99. The difficulty with this transition is that Mg^0 is not the dominant ionization state of Mg in a neutral hydrogen gas region; it has an ionization potential IP $<$ 13.6 eV. Therefore, the population of this ionization state is sensitive to a variety of physical conditions all of which are largely unconstrained by our observations. While another strong Mg I transition does exist at 2796Å, our observations never cover this profile. In short, those systems which have absorption profiles spanning over 50 km/s should be considered to have $N(\mathrm{Zn}^+)$ values with upper limits until Mg^0 is carefully considered.

An excellent example of this issue is presented by the damped system at $z = 1.776$ toward Q1331+17 (Paper I, § 3.20). Pettini et al. (1994) noted a significant feature in the Zn II 2026 profile which coincides with the Mg I 2026 transition and corrected $N(\mathrm{Zn}^+)$ accordingly. At higher resolution, however, we find that this absorption also coincides with a significant feature in the Fe II profiles meaning it could be another component in the Zn II profile, not Mg I. Even more confusing is the fact that the $N(\mathrm{Zn}^+)$ values for Zn II 2026 and 2062 agreed very well in our initial analysis (PW99). After performing a line-profile fitting analysis of all of the Cr II and Zn II profiles, however, we derived an $N(\mathrm{Zn}^+)$ value ≈ 0.05 dex lower than our previous analysis and a much lower $N(\mathrm{Mg}^0)$ value than that inferred by Pettini et al. In this case, therefore, correcting for Mg^0 suggests a significant underestimate of Zn^+ in the moderate resolution analysis but implies our initial echelle analysis provided a small overestimate to $N(\mathrm{Zn}^+)$.

An unequivocal example of Mg I 2026 absorption in our sample is in the damped Lyα system at $z_{abs} = 2.040$ toward Q0458−02. Figure 4 presents the Zn II 2026, Mg I 2026, and Cr II 2026 profiles as well as the Cr II 2056,

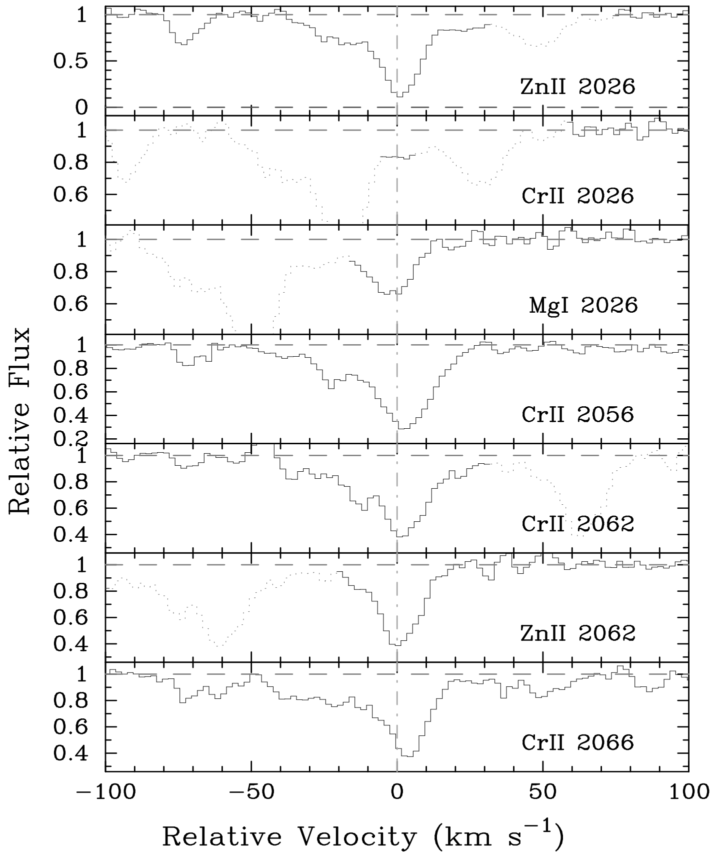

FIG. 4.— Metal-line profiles of the Zn II and Cr II transitions near 2025Å and the Mg I 2026 transition for the damped Lyα system toward Q0458–02. A comparison of the profiles provides convincing evidence that the feature at $v = 50$ km s^{-1} in the Zn II 2026 profile is not Zn^+ absorption but is due to Mg I 2026. Similar blending must be considered when measuring $N(Zn^+)$ from the Zn II 2026 transition. It is also possible, although far less certain, that we identify absorption due to Cr II 2026.

Cr II 2062, and Zn II 2062 transitions for this system. It is clear that the strong component at $v = 0$ km/s in the Mg I profile must be attributed to Mg^0 and not Zn^+. If we assume that the Mg I profile tracks the low-ion profiles (an assumption which need not hold), then the Mg I profile at $v < 50$ km s^{-1} contributes $\approx$4 mÅ to the Zn II 2026 equivalent width. This would imply a 0.025 dex enhancement to $N(Zn^+)$ in the linear limit of the curve of growth but more likely corresponds to a $\approx$0.020 dex correction. In Paper I we revised our $N(Zn^+)$ measurement downward by 0.02 dex from the value reported in PW99 to account for this blending. In Table 1, we list all of the systems in our analysis with Zn^+ measurements, note the likelihood of Mg I/Zn II line-blending, estimate a correction to $N(Zn^+)$, and indicate whether this correction was applied. In general, unless we identified clear evidence for the presence of Mg I, we chose not to apply any correction to $N(Zn^+)$. In the future, we will update the values in our online database as measurements of the Mg I 2796 profile are obtained.

Figure 5 presents the [Zn/Fe] values vs. [Fe/H] for our complete sample. Essentially every system exhibits an enhanced Zn/Fe ratio. While there are a number of systems with [Zn/Fe] $\leq$ 0.3 dex which could be explained by nucleosynthesis (e.g. P00), there are several systems with [Zn/Fe] $>$ 0.4 dex which are highly suggestive of dust depletion. Although it could be small number statistics, four of the six systems with [Fe/H] > -1.5 dex exhibit large Zn/Fe ratios. Despite this, there is no significant linear correlation between [Zn/Fe] and [Fe/H] (but see § 3.3). The observed range of Zn/Fe ratios may indicate a significant range in dust-to-gas ratios in the damped Lyα systems from system to system or at least sightline to sightline as noted by Pettini et al. (1997). We warn, however, that a fraction of this scatter could be related to the line blending described above or stochastic Zn nucleosynthesis.

TABLE 1
ZN MEASUREMENTS

QSO	z_{abs}	ZnII/MgI Blending?	Estimated correction	$N(Zn^+)$ corrected?
PH957	2.309	no		
Q0149+33	2.141	no	...	
Q0201+36	2.463	?	...	no
Q0458–02	2.040	yes	0.02	yes
Q0841+12	2.375	no	...	
Q0841+12	2.476	no	...	
Q1210+17	1.892	no	...	
Q1215+33	1.999	no	...	
Q1223+17	2.466	no	...	
Q1331+17	1.776	yes	0.06	yes
Q2206–19	1.920	yes	?	no
Q2230+02	1.864	yes	?	no
Q2359–02	2.095	?	?	no

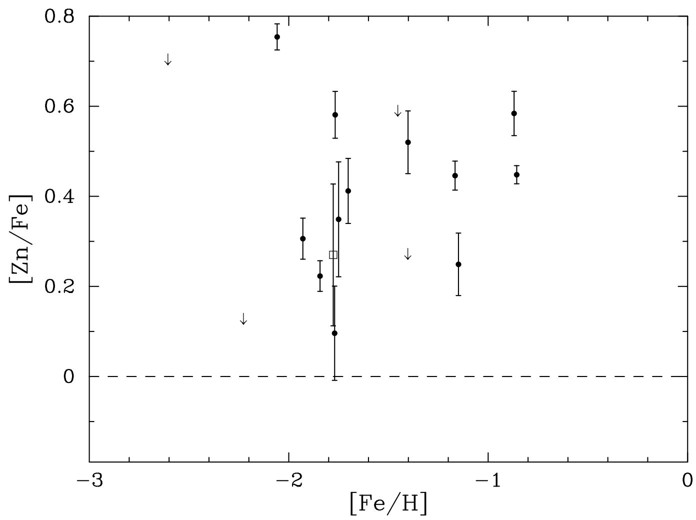

FIG. 5.— [Zn/Fe] abundance ratios vs. [Fe/H] metallicity for our complete sample of damped Lyα systems. Every system shows an enhanced value and there is no trend with metallicity. The dashed line at [Zn/Fe] = 0 indicates the solar meteoritic Zn/Fe ratio. The values plotted with a black square indicate that a proxy was substituted for Fe and an additional 0.05 dex error is being assumed.

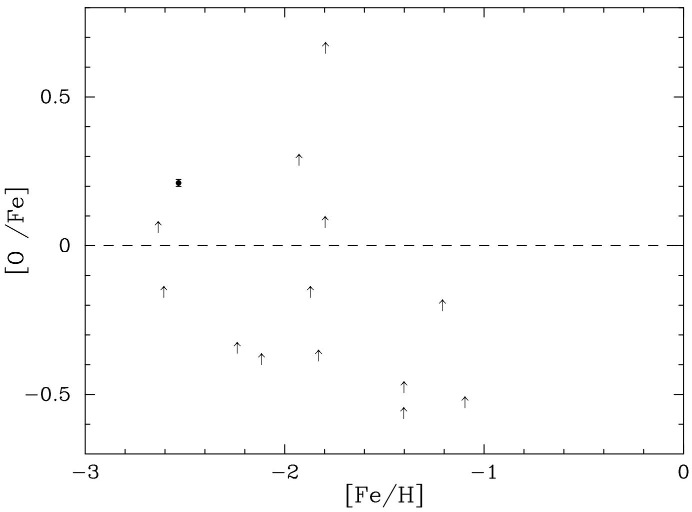

FIG. 6.— [O/Fe] abundance ratios vs. [Fe/H] metallicity for our complete sample of damped Lyα systems. With only one exception, all of the O I profiles are saturated in our damped Lyα systems and we only present lower limits on the O/Fe ratio. Only in the lowest metallicity systems do our [O/Fe] values begin to place meaningful constraints on the α-enrichment of the systems. Future observations with higher UV sensitivity should provide more measurements. The dashed line at [O/Fe] = 0 indicates the solar photospheric Ar/Fe ratio.

2.2. *Alpha Elements*

2.2.1. *Oxygen*

Oxygen is the prototypical α-element and its nucleosynthesis is dominated by Type II SN. Furthermore, it offers a particularly promising avenue for probing nucleosynthesis in the damped Lyα systems because it is only mildly refractory. Unfortunately, it is very challenging to observe oxygen in the damped systems; the majority of lines lie within the Lyα forest and tend to be heavily saturated. Molaro et al. (2000) have recently claimed a measurement of oxygen in the damped Lyα system toward Q0000−26 based on an analysis of the O I $\lambda\lambda$ 925,950 transitions. Adopting the Raassen & Uylings (1998) oscillator strength for Fe II 1611, these observations indicate an enhancement [O/Fe] $\approx +0.3$ dex consistent with values derived in metal-poor stars.

Figure 6 presents our sample of [O/Fe] measurements against [Fe/H] metallicity. With the exception of one system, all of our measurements on oxygen are lower limits. Unfortunately, only at the lowest [Fe/H] values do these limits begin to place meaningful constraints on the O/Fe ratio. The single measurement comes from the system at $z_{abs} = 2.844$ toward Q1946+76. L96 placed a lower limit on $N(\mathrm{O}^0)$ from the saturated O I 1302 transition, but our extensive wavelength coverage enables a measurement of $N(\mathrm{O}^0)$ from the O I 948 and 1039 transitions. The observed ratio, [O/Fe] $\approx +0.2$, indicates a modest enhancement. Surprisingly, the $N(\mathrm{O}^0)$ measurement also implies a sub-solar O/Si ratio which contradicts the observed trend in metal-poor stars (e.g. McWilliam et al. 1995). Perhaps this value is indicative of photoionization; Si^+ can arise in regions of photoionized gas. The other notable value is the lower limit on O/Fe for the system toward Q0336-01 ([O/Fe] = +0.6 dex which suggests an extremely α-enriched system.

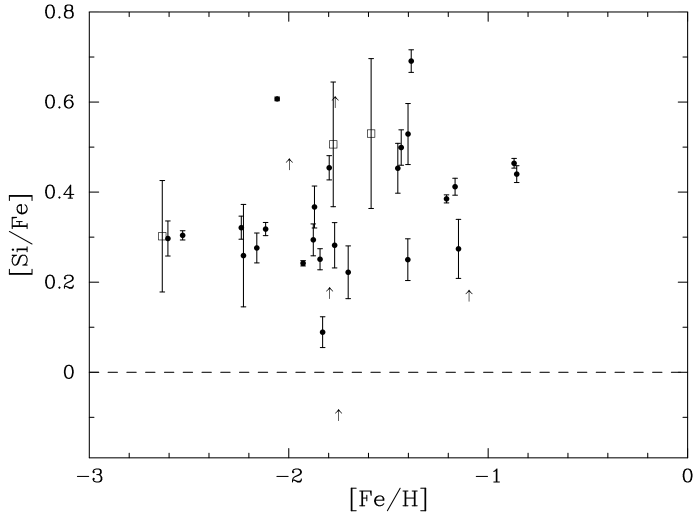

FIG. 7.— [Si/Fe] abundance ratios vs. [Fe/H] metallicity for our complete sample of damped Lyα systems. Every system shows an enhanced value and there is no trend with metallicity. The dashed line at [Si/Fe] = 0 indicates the solar meteoritic Si/Fe ratio. The values plotted with a black square indicate that a proxy was substituted for Fe and an additional 0.05 dex error is being assumed.

2.2.2. *Silicon*

With few exceptions, silicon represents the only α-element measurement for a given damped Lyα system. Although silicon is a refractory element, its depletion is mild in lightly depleted regions of the ISM and therefore the observed column densities for the damped Lyα systems should nearly reflect the total Si column density. Figure 7 plots the Si/Fe ratios against [Fe/H] metallicity for the 35 systems with a Si measurement. All of the damped Lyα systems show enhanced Si/Fe ratios with values ranging from +0.1 to +0.6 dex. Examining Figure 7, one notes the mean and scatter in the Si/Fe ratios exhibit little variation with [Fe/H] except that the systems at [Fe/H] < -2 dex show nearly constant Si/Fe ratios. The mean [Si/Fe] enhancement is similar to that for [Zn/Fe] which has led several authors to argue for a nearly solar Si/Fe ratio when dust depletion is taken into account (e.g. Vladilo 1998). As discussed in greater detail in § 4, however, we contend most systems exhibit a nucleosynthetic Si/Fe enhancement suggestive of Type II SN enrichment.

2.2.3. *Sulfur*

Sulfur is one of the truly non-refractory elements in the ISM, therefore it provides an unambiguous probe of nucleosynthesis. Figure 8 presents our complete sample of measurements. Like silicon, the S/Fe ratios are modestly enhanced in all cases.

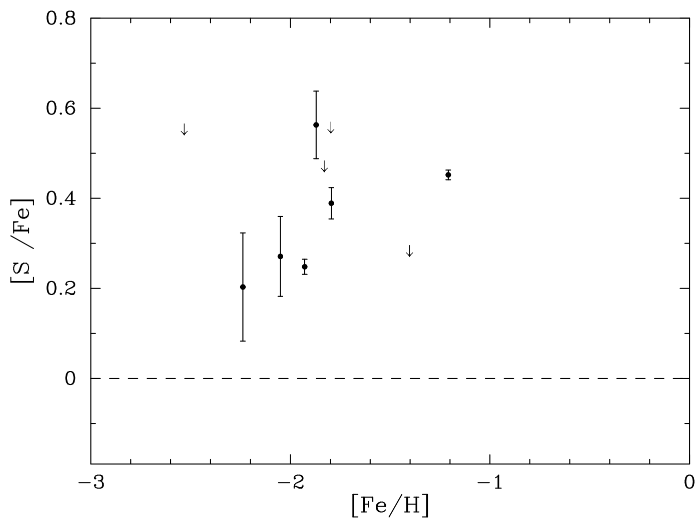

FIG. 8.— [S/Fe] abundance ratios vs. [Fe/H] metallicity for our complete sample of damped Lyα systems. Every system shows an enhanced value and there is no obvious trend with metallicity. The dashed line at [S/Fe] = 0 indicates the solar meteoritic S/Fe ratio.

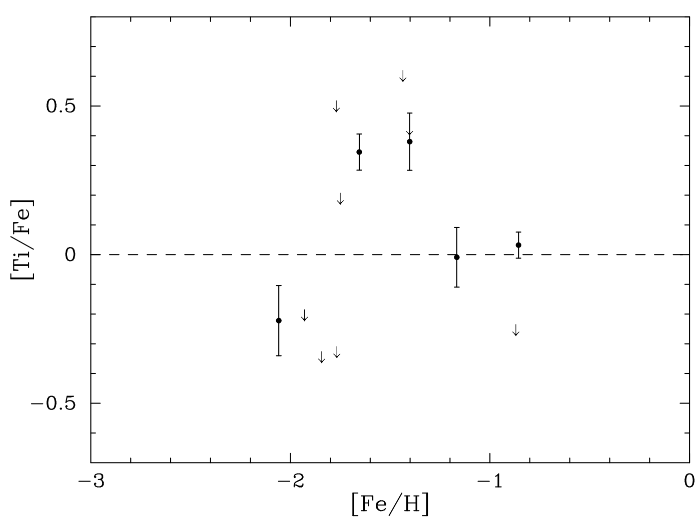

FIG. 9.— [Ti/Fe] abundance ratios vs. [Fe/H] metallicity for our complete sample of damped Lyα systems. The systems exhibit a range of values including several sub-solar upper limits which are indicative of dust depletion. The dashed line at [Ti/Fe] = 0 indicates the solar meteoritic Ti/Fe ratio.

2.2.4. *Titanium*

On theoretical grounds, Ti is expected to track Fe or even exhibit sub-solar abundances in the Galaxy (e.g. Timmes, Woosley, & Weaver 1995). Empirically, however, Ti generally tracks the other α-elements with enhancements relative to Fe of $\approx +0.3$ dex in metal-poor stars (McWilliam et al. 1995, P00). In the ISM, Ti either tracks Fe or is deficient relative to Fe (Savage et al. 1992; Howk, Savage, & Fabian 1999). Significant departure of Ti/Fe from the solar ratio, therefore, should provide unambiguous evidence for either nucleosynthesis or dust depletion.

Figure 9 presents our new and revised [Ti/Fe] values against [Fe/H]. For the few systems with measurements, the values scatter about the solar ratio. Having corrected for the oscillator strengths from PW99 (Wiese, Fedchak, & Lawler 2001), we no longer find significant evidence for an enhancement of Ti/Fe in the damped Lyα systems. In fact, the most striking aspect of Figure 9 is the set of three upper limits with [Ti/Fe] < -0.3 dex which suggest significant dust depletion. In one case (Q1223+17), however, the observed Zn/Fe ratio is small ([Zn/Fe] $\approx +0.2$ dex) and the system is unlikely to be severely depleted. Although it is a single example, one must be cautious in interpreting the low Ti/Fe ratios solely in terms of dust depletion.

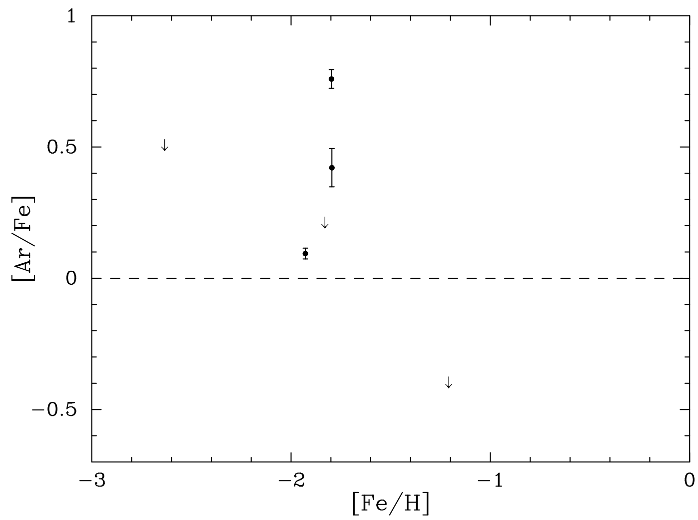

FIG. 10.— [Ar/Fe] abundance ratios vs. [Fe/H] metallicity for our complete sample of damped Lyα systems. The majority of systems show solar or enhanced Ar/Fe ratios suggestive of Type II SN enrichment and/or dust depletion. The dashed line at [Ar/Fe] = 0 indicates the solar photospheric Ar/Fe ratio.

2.2.5. *Argon*

Although argon is presumed to track the other α-elements, there is little empirical evidence. Argon is rarely observable in stellar atmospheres but it does trace O and S in metal-poor H II regions (Henry & Worthey 1999). Unfortunately, our observations provide measurements on Ar for only a limited number of systems. Figure 10 plots these observations against [Fe/H] metallicity. In agreement with the result presented by Molaro et al. (2001) for Ar in the system toward Q0000–26, several of our systems show enhanced Ar/Fe ratios. Because Ar is not depleted onto dust grains, the enhanced Ar/Fe values could reflect dust depletion, but they are also suggestive of significant Type II SN enrichment.

Following the conclusions of Sofia & Jenkins (1998) for the ISM, Molaro et al. (2001) noted that an observed solar or super-solar Ar/Si ratio significantly limits the level of photoionization in a given damped Lyα system. This is due to the fact that Ar is far more sensitive to photoionizing radiation than Si. Applying this axiom to the systems presented in Figure 10, we infer that the majority have low levels of photoionization (Figure 11). For the system

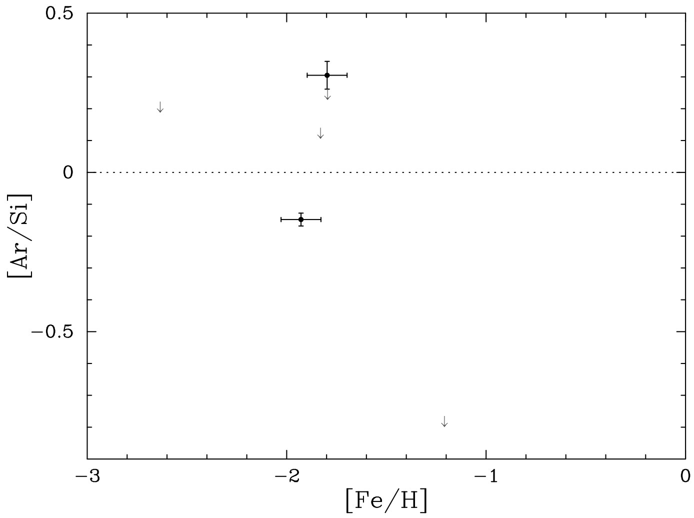

FIG. 11.— [Ar/Si] abundance ratios vs. [Fe/H] metallicity for our complete sample of damped Lyα systems. The Ar/Si ratio is an indicator of photoionization in gas-phase measurements with significant sub-solar values indicating photoionized gas. For the six damped systems with Ar observations, five are consistent with very little photoionization, while the system toward Q1759+75 is likely to be partially ionized. The dashed line at [Ar/Si] = 0 indicates the solar photospheric Ar/Si ratio.

toward Q1759+75, however, we note an an upper limit on Ar/Si which is significantly sub-solar. We interpret this value as an indication of substantial photoionization and discuss the implications in a future paper.

2.3. *Light Elements*

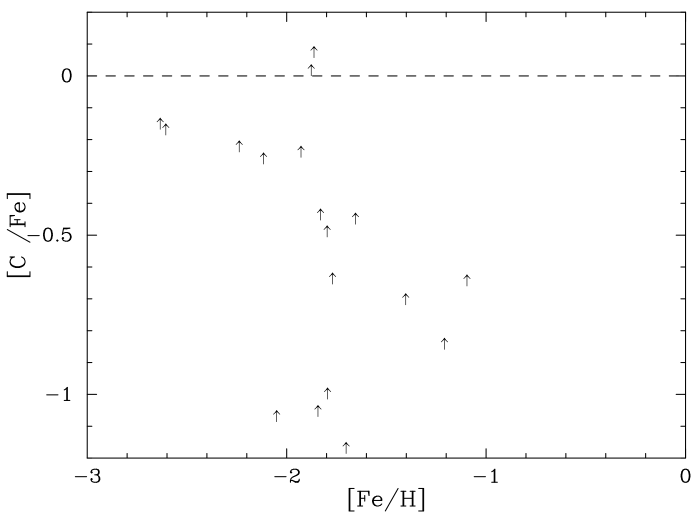

FIG. 12.— [C/Fe] abundance ratios vs. [Fe/H] metallicity for our complete sample of damped Lyα systems. We only report lower limits on C/Fe, the majority of which are too low to provide meaningful constraints on nucleosynthesis or dust depletion. The two systems with [C/Fe] > 0, however, are suggestive of significant dust depletion and/or photoionization. The dashed line at [C/Fe] = 0 indicates the solar photospheric C/Fe ratio.

2.3.1. *Carbon*

Because [C/Fe] is approximately solar in the majority of Galactic stars (Carretta, Gratton, & Sneden 2000; but see Wallerstein et al. 1997) and because carbon is mildly refractory, it can place unique constraints on interpretations of the damped Lyα abundance patterns. Specifically, carbon can act as a tracer of the Fe-peak which is unaffected by dust depletion. It is very unfortunate, then, that the two UV C II transitions are typically too strong to yield a meaningful limit on C/Fe. Figure 12 plots all of the C/Fe lower limits from our observations. We note two systems with [C/Fe] > 0: the system toward BRI0952–01 and the system at $z_{abs} = 2.154$ toward Q2359−02. In the case of the system toward BRI0952–01, the C II 1334 profile spans over 300 km/s and more resembles the C IV profiles than most other damped Lyα systems (Wolfe & Prochaska 2000). Because C^+ is present in partially ionized regions, we are concerned that this C II profile derives from gas in multiple phases. Unfortunately we do not have coverage for enough other low-ion profiles (e.g. Si II, Al II) to more accurately assess this presumption. For the system toward Q2359–02, the S/N of the C II 1334 profile is poor, but the profile is heavily saturated and [C/Fe] > +0.2 dex is possible. In this case, the C/Fe ratio may indicate dust depletion.

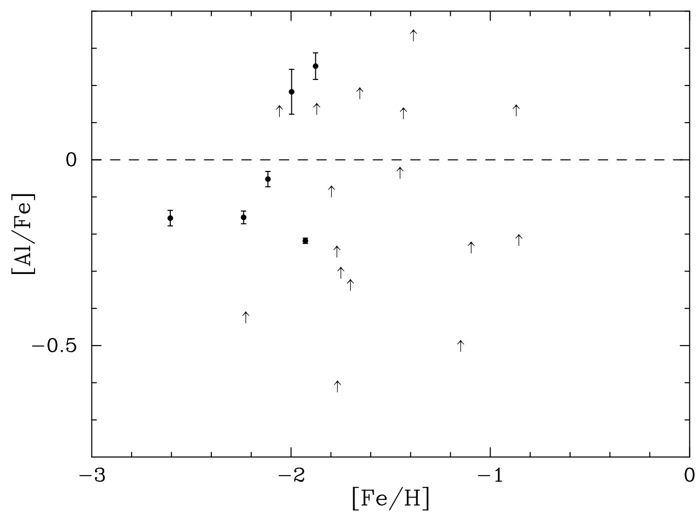

FIG. 13.— [Al/Fe] abundance ratios vs. [Fe/H] metallicity for our complete sample of damped Lyα systems. We report lower limits for the majority of systems including several super-solar values. Although it is difficult to assess a trend with metallicity, we contend that there is an increase in Al/Fe with increasing [Fe/H]. The dashed line at [Al/Fe] = 0 indicates the solar meteoritic Al/Fe ratio.

2.3.2. *Aluminum*

Al II 1670 is the strongest metal-line transition (highest λf-value) which we observe in the damped Lyα systems. For this reason, it can provide a metallicity diagnostic for even the most metal-poor systems. In the majority of systems, however, the profile is heavily saturated and we place only a lower limit on the Al/Fe ratio. Figure 13 presents all of the [Al/Fe] measurements and lower limits

Table 2
ELEMENT OVERVIEW

Element	Nucleo. Type	Galactic Stellar [X/Fe]		Galactic Dust [X/Fe]			Observing in DLA
		[Fe/H] = −2	[Fe/H] = −1	Nature	(Halo)	(Disk)	
C	Light element	0.0	0.0	mildly refractory	+0.5	+1.7	Saturated transtisions
O	α element	+0.4	+0.4	mildly refractory	+0.5	+1.7	Saturated transitions
Al	Odd-Z element	–1.0	0.0	refractory	0.0	0.0	Very strong transition
Si	α element	+0.3	+0.3	mildly refractory	+0.3	+1.0	
P	Odd-Z element	N/A	N/A	mildly refractory	+0.5	+1.5	Weak, Lyα Forest
S	α element	+0.5?	+0.3?	non-refractory	+0.6	+2.0	
Ar	α element?	N/A	N/A	mildly refractory	+0.5	+1.7	Lyα Forest
Ti	α element	+0.4	+0.4	refractory	0.0	–0.8	Weak transitions
Cr	Fe-peak element	–0.3	0.0	refractory	+0.1	0.0	
Co	Fe-peak element	+0.3	0.0	refractory	?	0.0	
Ni	Fe-peak element	0.0	0.0	refractory	0.0	– 0.2?	
Zn	?	+0.2	+0.1	mildly refractory	+0.6	+1.4	

against metallicity. At [Fe/H] < -2 dex, several of the damped Lyα systems show deficient Al/Fe ratios. In contrast, there are a number of lower limits with [Al/Fe] $\gtrsim 0$ at [Fe/H] > -1.5 including several where the Al II profile is heavily saturated. In these cases the [Al/Fe] values are probably at least +0.3 dex. Although the refractory nature of Al is not well established (Howk & Savage 1999), we note that the Al/Fe enhancements at [Fe/H] $\gtrsim -1.5$ and the underabundance of Al/Fe at [Fe/H] < -2 follow the general trends observed for metal-poor stars (McWilliam 1997).

2.4. *Summary*

In Table 2, we present a summary of all of the elements analyzed in the damped Lyα systems from our database to help the reader negotiate the following sections on dust depletion and nucleosynthesis. Column 1 lists the element, column 2 describes the dominant nucleosynthetic characteristic, columns 3 and 4 give the approximate [X/Fe] values in Galactic halo stars with [Fe/H] ≈ -2 and –1 dex respectively, columns 5–7 detail the refractory nature of each element and present rough [X/Fe] values in the warm halo and cool disk gas of the Galactic ISM, and column 8 comments on any difficulties associated with measuring the element in damped Lyα systems.

Table 3 provides a summary of the abundance measurements for the entire sample. Column 1 lists element X, column 2 details the number of systems (n) with measurements of X, column 3 gives the mean [X/Fe] ratio $\bar{x}$, column 4 is the scatter in the mean $\sigma(\bar{x})$, column 5 presents the median [X/Fe] value $\tilde{x}$, column 6 lists Pearson's r-value, and column 7 gives the probability of the null hypothesis (i.e. no linear correlation) from the Pearson test.

Table 3
ABUNDANCE SUMMARY

X	n	$\bar{x}$[a]	$\sigma(\bar{x})$	$\tilde{x}$[b]	r_{Pears}	P_{Pears}
C	0	...	...			
O	1	0.211	...			
Al	6	−0.025	0.196	−0.103	0.513	0.298
Si	26	0.379	0.166	0.320	0.305	0.130
P	1	0.198	...			
S	6	0.354	0.138	0.330	0.596	0.212
Ar	3	0.425	0.333	0.421	0.854	0.348
Ti	5	0.105	0.254	0.032	0.187	0.764
Cr	16	0.166	0.147	0.154	−0.177	0.512
Co	1	0.254	...			
Ni	25	0.057	0.135	0.094	0.462	0.020
Zn	13	0.450	0.217	0.446	0.014	0.963

[a] Mean
[b] Median

3. DUST DEPLETION

Every sightline through the ISM exhibits evidence for the presence of dust grains and there are many indications of dust in high redshift galaxies (e.g. Steidel et al. 1998; Richards 1999). For these reasons, one expects that the damped Lyα systems might also contain dust and exhibit at least modest levels of dust depletion. The damped Lyα systems are metal-poor and their observed abundance patterns presumably arise from the combination of a non-solar nucleosynthetic pattern and a dust depletion pattern. The challenge one faces is to disentangle the two patterns in order to gauge the implications of dust depletion and reveal the chemical enrichment history of these protogalaxies.

For the damped Lyα systems, the observed Zn/Fe (or Zn/Cr) enhancements have been identified as the most compelling argument that the refractory elements suffer at least modest levels of dust depletion (e.g. Pettini et al. 1994). Although this argument was well-founded initially, recent studies on Zn have challenged this presumption (Johnson 2001; Prochaska & Wolfe 2000; Primas et al. 2000; Umeda & Nomoto 2001). In short, our empirical and theoretical understanding of the nucleosynthesis of Zn may be sufficiently clouded that an enhanced Zn/Fe ratio on its own is not a definitive argument for the presence of dust depletion. To best address the issue of dust depletion, one must consider other ratios and search for additional

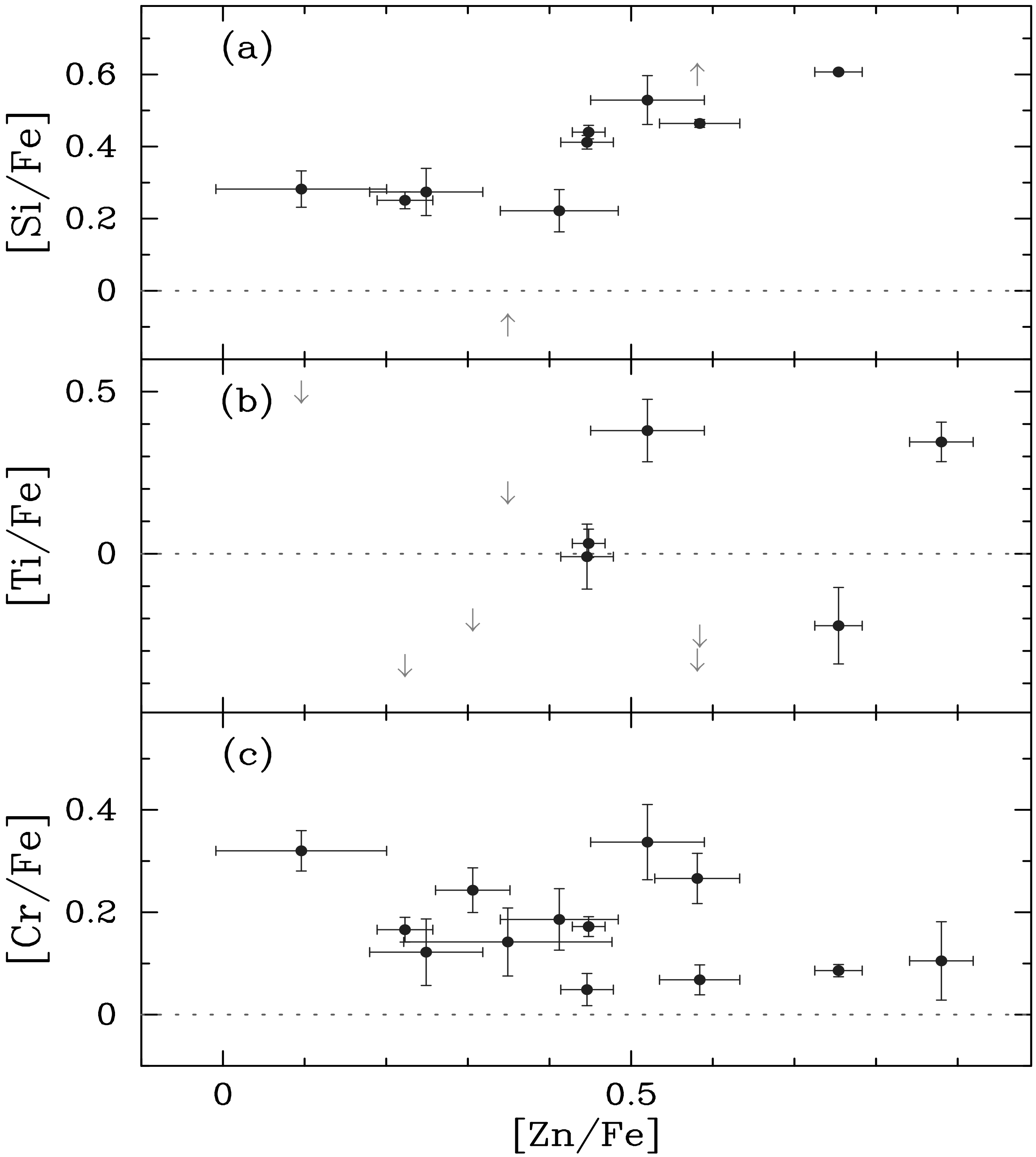

Fig. 14.— [X/Fe], [Zn/Fe] abundance ratio pairs for our sample of damped Lyα systems for (a) Si, (b) Ti, and (c) Cr. If [Zn/Fe] enhancements indicate significant dust depletion, one might expect trends for several of these X/Fe ratios.

abundance trends (e.g. Si/Fe vs. Zn/Fe; PW99). Nevertheless, examining new element ratios and trends can help break this degeneracy. This is the approach we take in the following sub-sections. To help guide the reader, Table 5 presents a summary (§ 4.5) of some of the most important abundance ratios in discussing dust depletion.

3.1. *[X/Fe] vs. [Zn/Fe]*

Figure 14 presents X/Fe ratios for (a) Si, (b) Ti, and (c) Cr against [Zn/Fe]. Although nucleosynthesis processes might yield Zn/Fe enhancements of +0.1 to +0.3 dex, we contend that larger enhancements are indicative of dust depletion. Therefore, if one observes X/Fe departures from the solar abundance ratio which are to be explained by dust depletion then one might expect a correlation (or anti-correlation) with [Zn/Fe]. In PW99, for example, we noted a correlation between the Zn/Fe and Si/Fe ratios and presented this correlation as tentative evidence for dust depletion in the systems with the largest ratios. The enlarged database has strengthened the significance of this correlation (Figure 14b); the Pearson's probability of the null hypothesis for no linear correlation is $P_{Pears} < 0.5\%$. Because one observes a similar trend along ISM sightlines, the correlation is suggestive of dust depletion.

Previous studies have noted enhancements of Cr/Fe in the majority of damped systems (L96; PW99). With the revised Fe II oscillator strengths, the median enhancement is even higher: $\tilde{x}$(Cr) =+0.17 dex. At present, there is no stellar population which exhibits an enhanced Cr/Fe ratio relative to solar. In fact, the extreme metal-poor stars tend to show deficient Cr/Fe (McWilliam et al. 1995), a trend which might be explained by Type II SN enrichment with a deep mass cut (Umeda & Nomoto 2001). In contrast, the majority of Galactic ISM sightlines show super-solar Cr/Fe ratios of $\approx +0.05 - 0.2$ dex (Savage & Sembach 1996). Therefore, one would tend to interpret the damped Lyα Cr/Fe enhancements in terms of dust depletion. With this hypothesis, one might expect the Cr/Fe and Zn/Fe enhancements to correlate. In the ISM, however, there is actually an anti-correlation where the less depleted warm halo sightlines exhibit the largest Cr/Fe ratios and the dense, highly depleted cold disk sightlines show solar Cr/Fe ratios (Savage & Sembach 1996). This trend is interpreted as occurring because Fe is more readily depleted into dust grain cores while Cr is more efficiently adsorbed into the grain mantles which form in denser, more depleted regions. Figure 14c plots [Cr/Fe] vs. [Zn/Fe] for the 12 systems in our sample and reveals no apparent trend between these two ratios: $r_{Pears} = -0.32, P_{Pears} = 31\%$. We note, however, that the systems with the lowest [Cr/Fe] values have relatively large [Zn/Fe] ratios. This point is accentuated by Figure 15 which compares (a) [Cr/Fe] and (b) [Cr/Ni] against [Zn/Cr]. Here, the systems exhibit an anti-correlation which follows the general trend of the ISM but at much lower levels of dust depletion. The quantitative difference is significant; Cr/Fe remains enhanced in the ISM until [Zn/Fe] $\approx +2.0$ dex. This difference suggests the damped Lyα trend may not be entirely due to dust depletion. A nucleosynthetic variation in the production of Cr *independent* of the production of Zn, Ni, and Fe could contribute significantly to the trends in Figure 15 where Cr is reported in both the abscissa and ordinate. Not

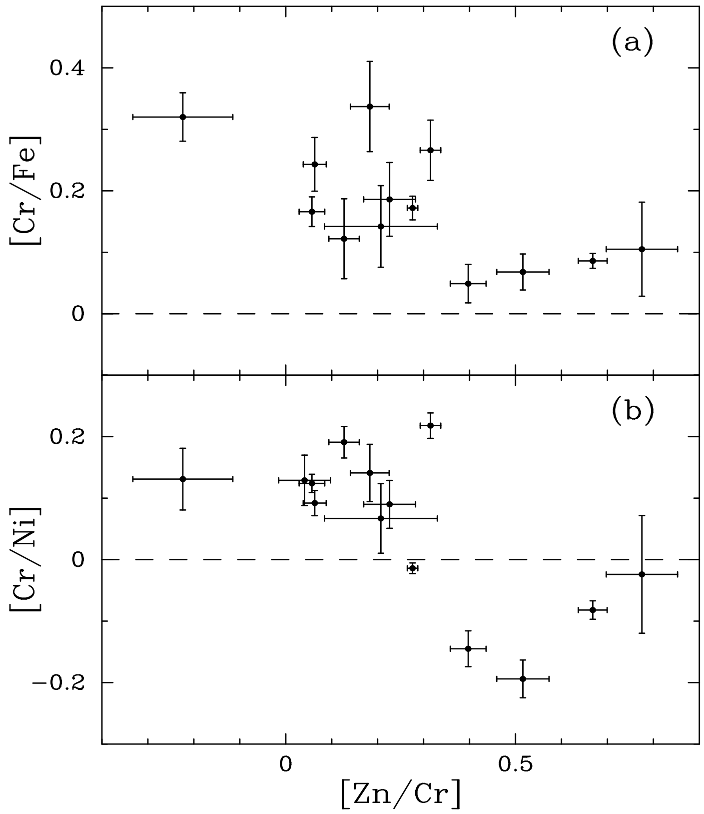

FIG. 15.— Plots of (a) [Cr/Fe] and (b) [Cr/Ni] vs. [Zn/Cr] for our complete sample of damped systems. In both panels we note a significant trend for decreasing [Cr/X] with increasing [Zn/Cr]. We suspect the trends are the combination of nucleosynthesis of Cr independent of the Fe-peak elements and dust depletion.

only could a nucleosynthetic process reproduce the anti-correlation, it could naturally explain the systems with large Cr enhancements at [Zn/Fe] ≈ 0.

The Ti/Fe ratio is significantly enhanced in the majority of metal-poor stars whereas Ti is often more heavily depleted than Fe in the ISM. Because of these competing trends, a significant offset in the Ti/Fe ratio from the solar value would pose strong evidence for one or the other process. As Figure 9 indicates, the damped Lyα systems generally show deficient Ti/Fe and several cases exhibit sub-solar upper limits: [Ti/Fe] < -0.3 dex. Because these Ti/Fe ratios contradict the empirical values for every star analyzed, they argue for significant dust depletion. Values of [Ti/Fe] ≤ -0.3 are generally observed only in severely dust depleted regions of the ISM (e.g. ζ Oph; but see Howk et al. 1999). Again, if the deficient Ti/Fe ratios are indicative of dust depletion, one might expect an anti-correlation between [Ti/Fe] and [Zn/Fe]. Examining Figure 14b, we note no obvious anti-correlation. Although several of the systems with large [Zn/Fe] values show low Ti/Fe ratios, the system with the largest [Ti/Fe] value also has a large Zn/Fe enhancement. If the sub-solar Ti/Fe ratios are indicative of dust depletion, then the results in Figure 14 suggest significant contributions to the Ti/Fe ratios from both nucleosynthesis and dust depletion.

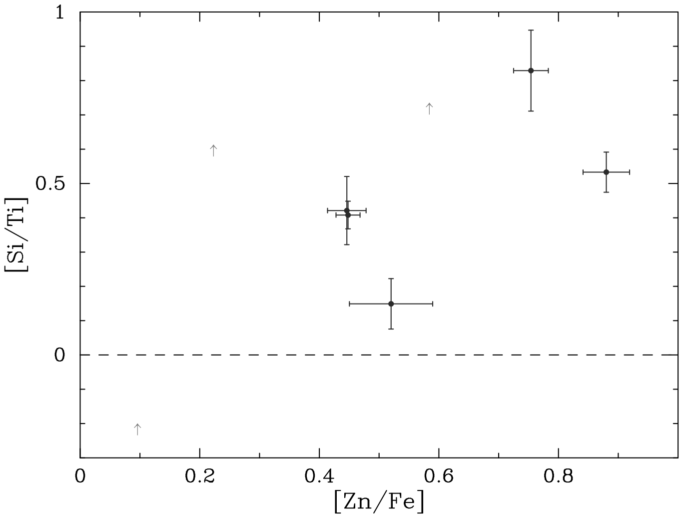

FIG. 16.— [Si/Ti] values plotted against [Zn/Fe] ratios in the few damped systems where all four elements have been observed. With the exception of one measurement and one lower limit, the systems show significantly enhanced Si/Ti and the hint of a trend for larger [Si/Ti] at larger [Zn/Fe]. These results are in strong conflict with the ratios observed in stars of any metallicity and therefore provide strong evidence for dust depletion in the systems with large [Si/Ti] and [Zn/Fe].

In Figure 16, we present [Si/Ti] ratios against [Zn/Fe] for the handful of damped systems where all four elements have been observed. The results are stunning. All of the systems are consistent with enhanced Si/Ti ratios and there is the hint of increasing [Si/Ti] with increasing [Zn/Fe]. Empirically, this presents *the most unambiguous evidence for dust depletion in our database.* Although the relative abundances of the α-elements vary in stars, essentially no star of any metallicity shows [Si/Ti] $> +0.2$ and none exhibit [Si/Ti] $> +0.3$ dex. In contrast, the results in Figure 16 generally follow the behavior of these four elements due to dust depletion in the ISM. Although Figure 16 is comprised of just five measurements, the results offer persuasive evidence for dust depletion in damped Lyα systems with large Si/Ti ratios. We stress that future damped Lyα studies should concentrate on providing more measurements of Ti.

3.2. *[X/Y] vs. [Y/H]* + $\log N$(HI)

In a recent paper, Hou et al. (2001) presented an argument for dust depletion in the damped Lyα systems based on the anti-correlation between X/Zn ratios and F(Zn) $\equiv$ [Zn/H] $+ \log N$(HI) values which they culled from the literature. We present these quantities for several elements in Figure 17. Because Hou et al. (2001) included many measurements from PW99, it is not surprising that we find similar anti-correlations. We worry, however, that the observed trends might not result from dust depletion. As Hou et al. (2001) noted, an anti-correlation is observed in the ISM when X/Zn is considered against N(HI), presumably because higher N(HI) sightlines probe denser regions Wakker & Mathis (2000). In contrast, the damped Lyα systems do not exhibit trends between X/Zn and N(HI), but X/Zn and F(Zn) which is simply N(Zn) + 12.0 − 4.67. It is not obvious that the X/Zn ratios should anti-correlate with N(Zn). For example, sightlines with large N(HI) values but small [Zn/H] might have very different physical properties than sightlines with high [Zn/H] and low N(HI). We also have concerns that the observed X/Fe vs. F(Zn) trends could be due to variations in the production of Zn relative to the Fe-peak elements, in particular because the nucleosynthetic history of Zn is expected to be independent of the Fe-peak elements (e.g. Hoffman et al. 1996). Because the figure simply plots X/Zn vs. N(Zn), an anti-correlation could arise from a significant dispersion in the production of Zn either from galaxy to galaxy and/or within a given galaxy. Similarly, variations in N(Zn) from uncorrected line blending (§ 2.1.5) could enhance the anti-correlations.

TABLE 4
[X/Y] VS. [Y/H] + LOG(HI)

Y	X	n	r_{pears}	P_{pears}
Zn	Si	11	−0.600	0.051
	Ti	5	−0.099	0.874
	Cr	14	−0.604	0.022
	Fe	13	−0.550	0.052
	Ni	14	−0.582	0.029
Zn[a]	Si	10	−0.406	0.245
	Ti	5	−0.099	0.874
	Cr	13	−0.394	0.183
	Fe	12	−0.325	0.303
	Ni	13	−0.326	0.278
Si	Al	6	0.220	0.675
	Ti	5	0.100	0.873
	Cr	14	−0.666	0.009
	Fe	26	−0.498	0.010
	Ni	22	−0.742	0.000
	Zn	11	0.322	0.335
Si[a]	Al	6	0.220	0.675
	Ti	5	0.100	0.873
	Cr	13	−0.611	0.026
	Fe	25	−0.491	0.013
	Ni	21	−0.736	0.000
	Zn	10	−0.079	0.828

[a] Statistics do not include the system toward Q0149+33

Both the apparent and quantitative evidence for the anti-correlations in Figure 17 are driven by the single system toward Q0149+33. This system exhibits the lowest [Zn/H] $+ \log N$(HI) value in our sample and marks the detection limit of N(Zn$^+$) from a typical high resolution observation. Although we consider the relative abundance measurements for the Q0149+33 system to be reasonably accurate, we caution the reader against drawing significant conclusions from this single system. To emphasize the point, we present the probability for the null hypothesis

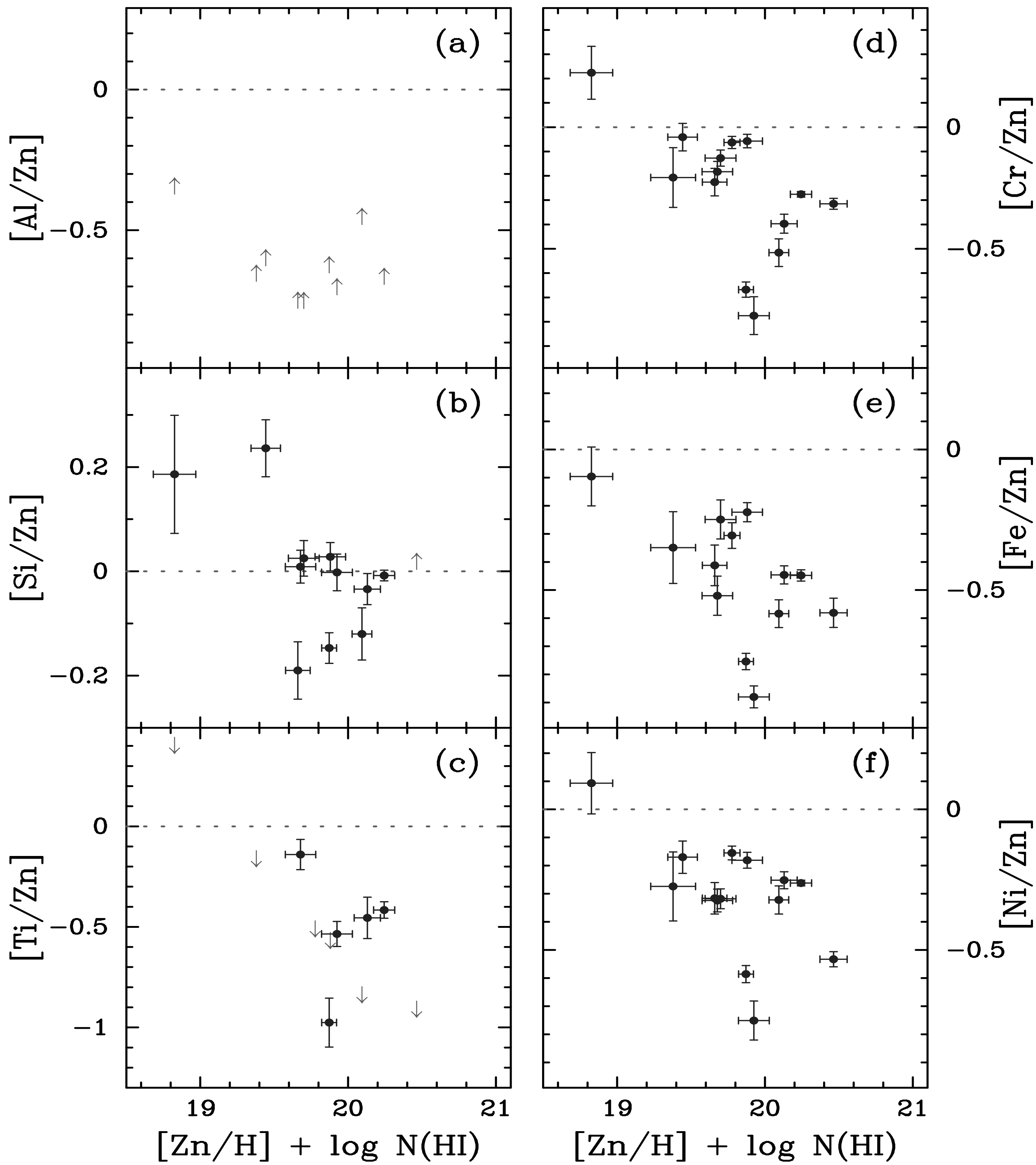

FIG. 17.— [X/Zn] vs. [Zn/H] + log(HI) for our complete sample of damped Lyα systems. The majority of elements exhibit the anti-correlation first identified by Hou et al. (2001). These anti-correlations disappear, however, if one removes the single system toward Q0149+33. As noted in § 5, the absence of systems with large [X/Zn] and [Zn/H] + log(HI) argues against dust obscuration.

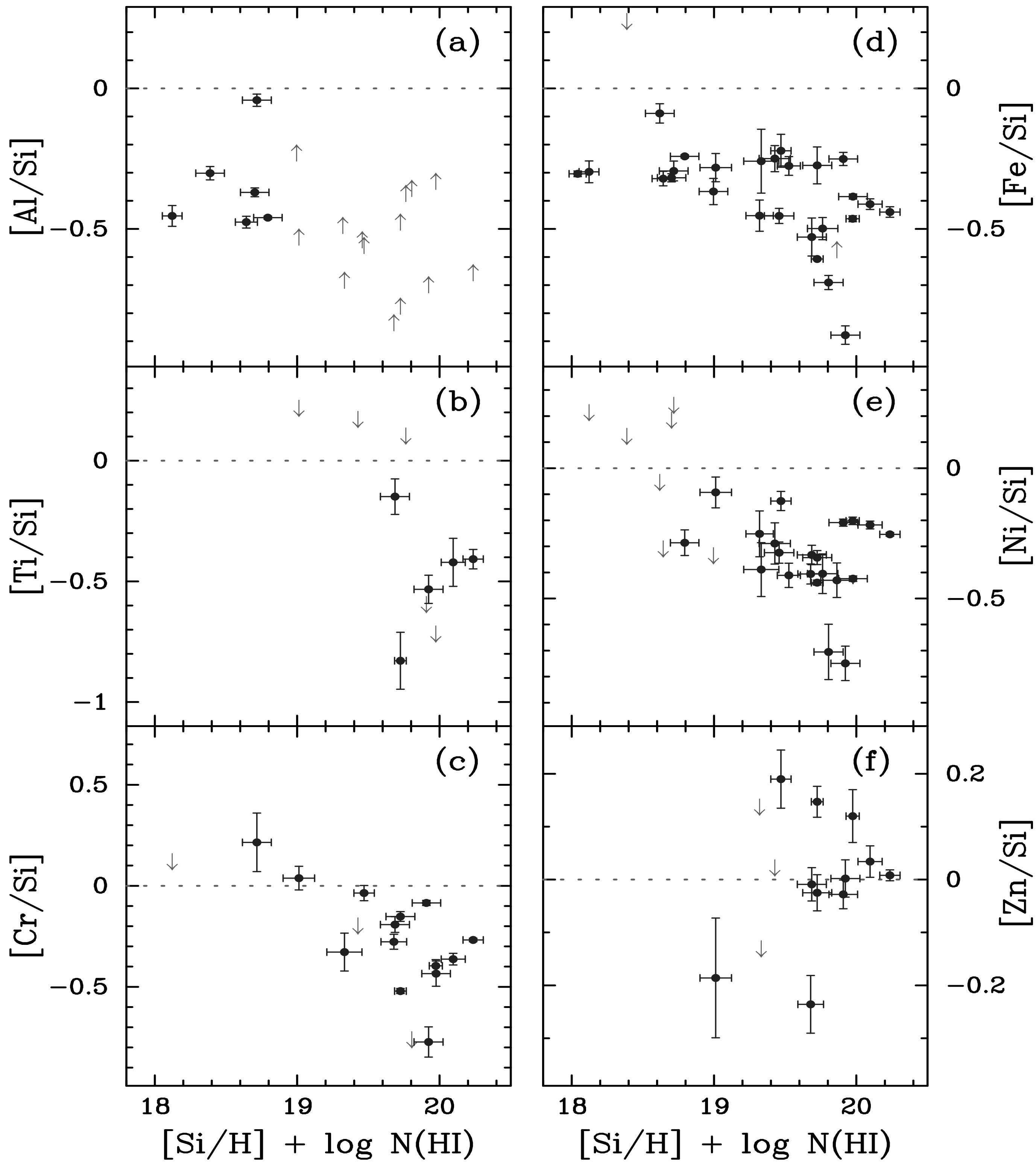

FIG. 18.— This figure is analogous to Figure 17 except we have substituted the roles of Si and Zn. In this case, we find statistically significant anti-correlations for almost all of the elements which argues for dust depletion in systems with large [Si/H] + log(HI).

of no linear correlation in Table 4 both including and remaining the damped system toward Q0149+33. Although most of the elements exhibit significant anti-correlations when Q0149+33 is included ($P_{Pears} < 5\%$), none have $P_{Pears} < 15\%$ when the system is removed. Obviously, a further examination of damped systems with very low N(Zn) values is required to establish or contradict these anti-correlations. This task is difficult, however, because one quickly approaches the detection limit of Zn.

In lieu of new Zn measurements, we can address the anti-correlations by considering the same analysis but replacing Zn with Si. Although Si is mildly refractory, the damped Lyα Si/Zn ratios are nearly solar and do not appear to correlate with [Fe/H], N(HI), or redshift. Therefore, we feel confident in substituting Si for Zn in this analysis. Figure 18 plots [X/Si] against F(Si) for the same elements presented in Figure 17. For Cr, Ni, and Fe there are statistically significant anti-correlations, none of which hinge on a single system (Table 4). In contrast to the analysis of Zn, the ratios do not decrease monotonically with increasing F(Si) but instead tend to exhibit a range of [X/Si] values at higher F(Si). This suggests that F(Si), i.e. N(Si), is not the dominant indicator of dust depletion. In the next section we argue that [Si/H] metallicity is the dominant predictor of dust depletion in the damped Lyα systems. Nevertheless, we contend the general decrease in [X/Si] is the result of dust depletion, as envisioned by Hou et al.

3.3. *[X/Y] vs. [Si/H]*

In § 2 we presented abundances for each element relative to Fe against the [Fe/H] metallicity, in large part to facilitate comparisons with the Galactic ISM and stellar abundances. We have concerns, however, that the effects of dust depletion may hide significant trends with metallicity if we compare against [Fe/H] instead of a much less refractory metallicity indicator. To illustrate this point, we plot several abundance ratios against [Si/H] in Figure 19. For systems with lower limits on $N(\mathrm{Si}^+)$, we plot the data points as right or diagonal arrows.

The results for several of the abundance ratios are striking. In particular, [Si/Fe] exhibits a strong dependence on [Si/H] (Figure 19a). The values are nearly constant for [Si/H] $= -2.5$ to -1 dex but increase by several tenths of a dex at higher metallicity. This trend is highly suggestive of dust depletion in the highest metallicity systems and argues that the plateau results from a nucleosynthetic 'floor' (see § 4.1). Furthermore, one draws a similar conclusion from the Si/Cr and Zn/Fe data points albeit at lower statistical significance. Altogether, the trends indicate depletion levels of a few 0.1 dex in the highest metallicity damped Lyα systems.

In contrast to the Si/Fe ratios, the Si/Ni ratios are reasonably constant over the entire range of metallicity. Furthermore, the systems with the highest two [Si/H] values actually exhibit two of the *lowest* [Si/Ni] values. The difference in the behavior of Ni and Fe is difficult to understand, particularly because dust depletion should imply even larger Si/Ni ratios. Although photoionization would tend to predict enhanced Ni/Fe ratios together with higher Si/Fe abundance, the low Ni/Cr ratios contradict this explanation (Howk & Sembach 1999). Maybe the Ni abundances imply a special nucleosynthetic process which yields super-solar Ni/Fe at high metallicity or possibly a dust depletion pattern different from the Galactic ISM. The disparity between Si/Fe and Si/Ni implies that Ni/Fe increases with [Si/H] which is partly indicated by Figure 19c. Although this trend is dominated by small number statistics, it will be very important to pursue this with future Ni measurements.

Finally, consider the S/Si ratios presented in Figure 19f. Nucleosynthesis generally predicts a solar relative abundance or perhaps modestly sub-solar S/Si ratios (Woosley & Weaver 1995). On the other hand, Si is readily locked into silicate dust grains and even the lightly depleted regions of the ISM exhibit [S/Si] $> +0.2$ (e.g. Savage & Sembach 1996). With the ISM as our guide, it appears very unlikely that Fe would be locked into grain cores without at least a modest depletion of Si. Examining Figure 19f, we note that none of the systems exhibit significantly super-solar S/Si ratios. By chance, all of the systems with S measurements have [Si/Fe] $\approx +0.3$ which matches the nucleosynthetic threshold implied by Figure 19a. Together the Si/Fe and S/Si ratios argue that very little Si is locked up in dust grains in these low [Si/H] damped systems and that the Si/Fe and S/Fe enhancements are simply the product of nucleosynthesis. Future S measurements of the significantly depleted damped systems (i.e. [Si/Fe] $> +0.5$) will allow for an investigation into the formation of silicates in the damped Lyα systems.

4. NUCLEOSYNTHESIS

For the same reasons it is difficult to identify abundance ratios which establish or rule out the presence of dust depletion in the damped Lyα systems, it is also challenging to reveal the underlying nucleosynthetic patterns. Not surprisingly, previous authors have offered competing viewpoints. L96 argued that the enhanced Si/Fe and S/Fe ratios and the sub-solar Mn/Fe ratios provide compelling evidence for Type II SN enrichment. At the time, they explained the enhanced Zn/Fe ratios in terms of nucleosynthetic enrichment which – at least in part – has been borne out by recent theoretical and empirical studies. In contrast, other authors have noted that if one corrects for dust depletion under the assumption that Zn/Fe is an accurate assessment of depletion, then the underlying nucleosynthetic pattern is more suggestive of solar abundances, i.e., enrichment dominated by Type Ia SN (Kulkarni et al. 1997; Vladilo 1998). As we discussed in PW99 and P00, the two viewpoints are difficult to reconcile, particularly because one observes enhanced Zn/Fe ratios in metal-poor stars. Until there is a major breakthrough in our understanding of dust depletion in the damped systems, the most fruitful approach is to consider abundance ratios which break the dust/nucleosynthesis degeneracy and/or damped systems where the abundance ratios suggest negligible dust depletion (Pettini et al. 1999; PW99; Molaro et al. 2000). We adopt this method in the following subsections, stressing several abundance patterns which reflect on nucleosynthesis largely independent of dust depletion. A brief summary of the most important points is presented in Table 5 (§ 4.5).

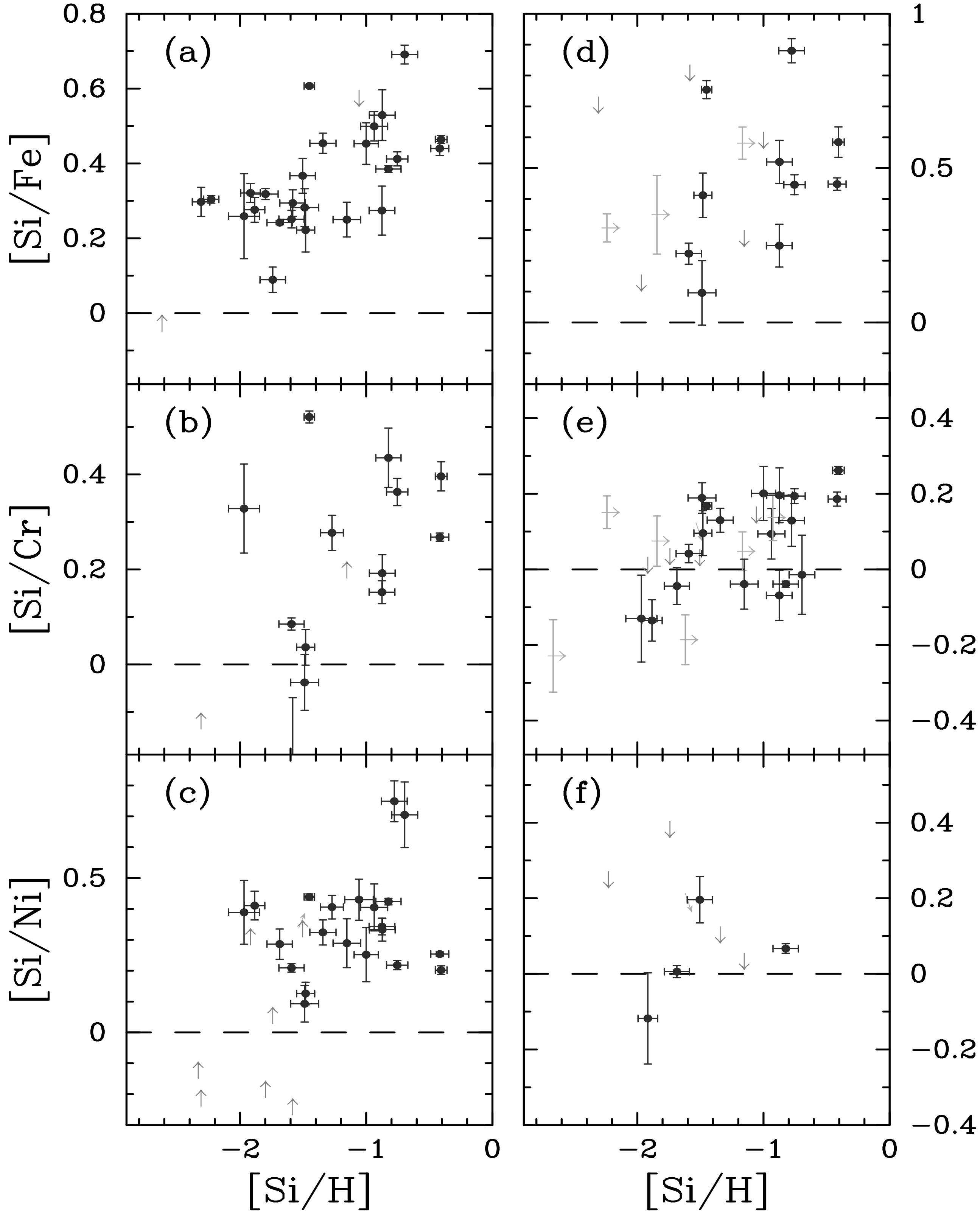

FIG. 19.— Relative abundance measurements for several select ratios plotted against [Si/H] metallicity. The lighter shaded data points and diagonal errors indicate those systems with lower limits to $N(\mathrm{Si}^+)$. We contend that the increase in [Si/Fe] with increasing [Si/H] is indicative of dust depletion. This interpretation is supported by similar trends for [Si/Cr] and [Zn/Fe]. We also note a plateau of [Si/Fe] values at [Si/H] < -1.3 which we argue is due to significant α-enrichment in the metal-poor damped Lyα systems.

4.1. *Investigating Type I vs. Type II SN Enrichment with [X/Fe] Ratios*

Si is the only α-element that is routinely measured in the damped Lyα systems. Figure 7 shows that every damped Lyα system exhibits enhanced [Si/Fe] and all but one has [Si/Fe] $\geq +0.2$ dex. Although it is difficult to separate the competing effects of dust depletion and nucleosynthesis on the Si/Fe enhancements, consider the following arguments. In Figure 14a, we noted that the Si/Fe enhancements tend to [Si/Fe] $\approx +0.25$ dex as [Zn/Fe] $\to 0$, i.e., in dust-free systems. This trend suggests the damped Lyα systems have α-enhancements of +0.2 to +0.3 dex although the argument is tentative because only a few systems have [Zn/Fe] ≈ 0. Our interpretation is substantiated, however, by the results presented in Figures 18a and 19a which plot [Fe/Si] and [Si/Fe] values against N(Si) and [Si/H] respectively. Here, the Si/Fe ratios have a nearly constant value of [Si/Fe] $\approx +0.3$ dex at [Si/H] < -1.5 and does not show larger values until [Si/H] > -1 where dust depletion is probably making a significant contribution. Together these trends imply the metal-poor damped Lyα systems are primarily enriched by Type II SN.

A Type II SN enrichment interpretation is further supported by the S/Si ratios. Because sulfur is non-refractory, one can use the difference in the refractory nature of S and Si to gauge the level of Si depletion, i.e., by searching for systematically large S/Si ratios. The absence of such a signature in Figure 19f argues that systems with low [Si/H] have no silicate dust grains and presumably are essentially dust-free. This further supports our contention that the Si/Fe enhancements in these systems result from nucleosynthesis and not dust depletion.

L96 and Prochaska & Wolfe (1997a) have stressed that Mn/Fe and Ti/Fe ratios can provide insight into the debate on Type II and Type Ia nucleosynthesis independent of dust depletion, but recent developments appear to limit the impact of these elements. First, recent abundance studies of the Sagittarius dwarf galaxy reveal sub-solar Mn/Fe abundances in stars with nearly solar α/Fe ratios (Smecker-Hane & McWilliam 2001) contrary to the majority of Galactic stars. If these results hold and are not an anomaly when compared with abundances of other dwarf galaxies, the impact of Mn in terms of nucleosynthesis will be reduced. Second our additional Ti measurements and the revised Ti II 1910 oscillator strengths indicate the majority of damped systems have solar or sub-solar Ti/Fe values. In these cases, it is difficult to comment on nucleosynthesis because the low Ti/Fe ratios are likely the result of dust depletion (e.g. Figure 16). Hopefully, the next generation of echelle spectrographs with higher UV sensitivity will yield a number of Ar measurements and more meaningful lower limits on $N(\mathrm{O}^0)$. These elements are nearly non-refractory and are important diagnostics of α-enrichment. In turn, comparisons among the α-elements provide insight into the enrichment histories of the damped Lyα systems as well as meaningful information on dust depletion.

4.2. *Comparisons Along the Fe-Peak*

In previous sections, we noted departures from the solar ratio for Cr/Fe and Ni/Fe which bear repeating. Specifically, nearly every damped Lyα system exhibits super-solar Cr/Fe and the majority show mild Ni/Fe enhancements. In terms of Cr, we suspect that dust depletion is playing a role in the relative abundances when [Zn/Fe] $>$ +0.3 (§ 3.1), but note that Cr/Fe is enhanced even in systems which are essentially dust-free (i.e. [Zn/Fe] ≈ 0). Furthermore, many of the [Cr/Fe] values are in excess of the highest values in the ISM (Savage & Sembach 1996). We contend these trends may have a nucleosynthetic origin. Furthermore, we suspect the anti-correlation observed between [Cr/Fe] and [Zn/Cr] (Figure 15) arises from a nucleosynthetic process. Although there is evidence in metal-poor stars for some differences among the Fe-peak elements, Cr/Fe is actually underabundant at low metallicities while [Ni/Fe] ≈ 0 at all metallicity. If these differences between the damped Lyα patterns and the Galactic stellar abundances hold, they may indicate important nucleosynthetic processes for Ni, Cr, and Fe which have not yet been appreciated. They could also reflect differences between gas-phase and stellar atmospheric abundances produced by differential supernova enrichment.

At present, Cr, Ni, and Fe are the best studied Fe-peak elements in the damped Lyα systems. There is some promise, however, to analyze Co in a number of systems (e.g. Ellison, Ryan, & Prochaska 2001). It will be particularly interesting to find if the damped systems show [Co/Fe] > 0 dex like metal-poor stars and if the Co abundances track Zn as suggested by Umeda & Nomoto (2001).

4.3. *Odd-Z Elements*

To date, aluminum has not received much attention in the damped Lyα systems except for its impact on the likelihood of photoionization (PW96; Howk & Sembach 1999; Vladilo et al. 2001). This light element, however, is special for being one of the few elements observed in damped systems with an odd atomic number. Determining the Al abundance is made difficult both by our limited knowledge of its refractory nature (Howk & Savage 1999) and its possible sensitivity to photoionization (Vladilo et al. 2001). Nevertheless, as noted in § 2.3.2, there may be a discernible trend of [Al/Fe] with [Fe/H] metallicity. In particular, a number of systems with [Fe/H] > -2 exhibit enhanced Al/Fe ratios while the few measurements with sub-solar Al/Fe are at [Fe/H] < -2. This trend loosely follows the behavior of Al in Galactic metal-poor stars (McWilliam 1997) and may reflect a similar nucleosynthetic history as well as a significant metallicity dependence to the production of Al relative to Fe.

Because Al is an odd-element, it is particularly valuable to compare its abundance with a nearby even-element (e.g. Si) in order to probe the so-called 'odd-even effect' (Arnett 1971). This effect refers to the higher relative abundance of elements with even atomic numbers because of the strong coupling (and therefore greater stability) of pairs of nucleons. Recent work on nucleosynthesis in zero metallicity stars indicates a strong odd-even effect in elements with Z < 25, for example, [Si/Al] $\gtrsim 1$ (Heger & Woosley 2001). Ideally, we could test these predictions with measurements of damped Lyα systems at [Fe/H] < -3, but it appears that no systems exist with these very low metallicities (§ 6). Instead, we must compare against scenarios which allow for at least one prior generation of star formation. Figure 20 plots [Si/Al] against [Fe/H] for our complete damped Lyα sample. Although the majority of systems have enhanced Si/Al, none have [Si/Al] ≈ 1. We emphasize that the refractory nature of Al suggests the [Si/Al] values might be *overestimates* of the intrinsic abundance. In fact, if one assumed that the Si/Fe enhancements are solely due to dust depletion and that Al has the same refractory behavior as Fe, then the dust-corrected [Si/Al] ratios would be approximately solar.

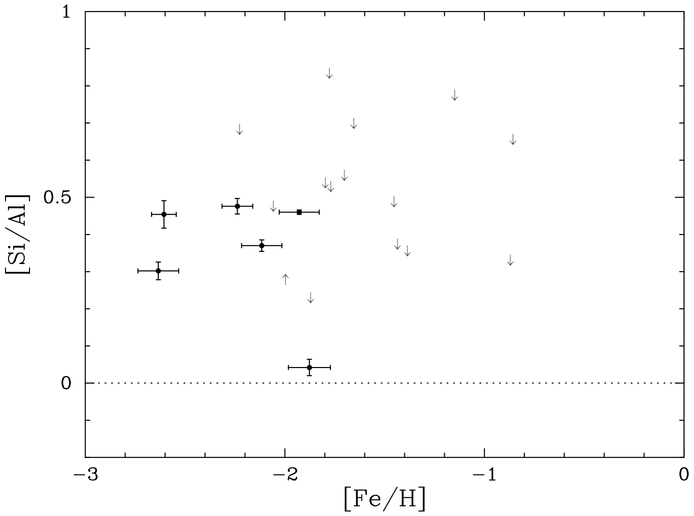

FIG. 20.— [Si/Al] values plotted against [Fe/H] metallicity. Contrary to predictions of nucleosynthesis and observations of Galactic metal-poor stars, the damped Lyα systems only show mildly enhanced Si/Al ratios. Furthermore, there is no trend in the values where one might have expected increasing Si/Al with decreasing [Fe/H]. The results suggest that the damped Lyα systems experienced a different chemical enrichment history from the Galactic halo.

Even without a dust-correction[5], the Si/Al ratios are lower than the Si/Al ratios of metal-poor stars with similar metallicity (McWilliam et al. 1995). Furthermore, the damped Lyα systems show no sign of increasing Si/Al with decreasing metallicity. In terms of Al, we contend that the damped Lyα systems have a different enrichment history than Galactic stars with [Fe/H] ≈ -2. Perhaps the differences indicate a greater contribution of lower mass supernovae in the damped Lyα systems. Another possibility is that the metals observed in the damped systems are the products of metal-rich star forming regions which have been diluted by primordial gas.

In passing, we note that one can also probe the odd-even effect through measurements of phosphorus. In comparison with aluminum, phosphorus is essentially non-refractory and should have negligible ionization corrections. Furthermore the P II 1152 transition has a smaller oscillator strength and will provide a number of measurements at higher metallicity where the Al II 1670 transition is always saturated. Therefore, future abundance studies should allow us to consider the odd-even effect over the full range of damped Lyα metallicities.

[5]The effects of photoionization might balance the effects of dust depletion (Vladilo et al. 2001)

4.4. *'Correcting' for Dust Depletion*

In this section, we have focused on abundance ratios relevant to the nucleosynthetic history of the damped Lyα systems which are largely independent of dust depletion. At the present time, we feel there is not enough information from the damped Lyα observations to allow for a quantitative analysis of dust depletion corrections. In particular, we have serious concerns about the assumptions of the dust depletion pattern and overall depletion level of the damped systems. For example, previous authors have simply assumed Zn/Fe is intrinsically solar and constrained their dust correction analysis accordingly. Because there may be a nucleosynthetic contribution to Zn/Fe, this implies an overestimate to these dust corrections. Although it is not very constructive, instead of presenting our own analysis we offer some criticism on treatments in the literature.

The most comprehensive approach to dust corrections in the damped Lyα systems was presented by Vladilo (1998). In his prescription, Vladilo assumed that dust in the damped Lyα systems has the same average number of atoms of each element per grain as Galactic dust. If, for example, Galactic dust has two Mn atoms depleted for every 10 Fe atoms, then this ratio applies for the damped Lyα systems *irrespective of the total number of Mn and Fe atoms present*. In other words, the dust grain composition (e.g. silicates, oxides) is independent of the relative quantities of the elements present during grain formation. Physically, one expects the two-body process of adhesion of an element onto dust grains to be proportional to the product of the densities of that element and the dust grains. If there are fewer atoms available (i.e. due to a nucleosynthetic underabundance), then the adhesion rate will be correspondingly lower. Aside from this assumption being non-physical, this treatment systematically reduces the observed departure from solar of any refractory element relative to Fe because the corrections are inversely proportional to the gas-phase abundances (see the Appendix). At some level, this treatment biases the analysis in favor of Vladilo's conclusion that the damped Lyα systems have solar relative composition. Until someone develops a more quantitative model of dust grain formation in the ISM, the practice of dust corrections will be too difficult to apply in detail to the damped Lyα systems.

4.5. *Summary of Dust Depletion and Nucleosynthesis*

This paper presents discussion and comparison on many relative abundance ratios for the damped Lyα systems to develop arguments for various aspects of dust depletion, nucleosynthesis, etc. In Table 5, we present an executive summary of these important abundance ratios.

5. DUST OBSCURATION

The prospect that extragalactic objects are obscured by dust was first stressed by Ostriker & Heisler (1984) and then thoroughly investigated for the damped Lyα systems by Fall & Pei (1993). The obvious concern regarding dust obscuration is that systems with significant dust extinction (e.g. highly depleted, high N(HI) systems) may drop from an optically selected quasar sample and therefore bias surveys against large N(HI) and/or possibly high metallicity systems (e.g. Boissé et al. 1998). In this section, we

TABLE 5
RATIO COMPARISON SUMMARY

Ratios	Trend	Nucleosynthesis	Dust Depletion	Comments
Si/Fe vs. Zn/Fe	Plateau + Correlation	Plateau at [Zn/Fe] $< +0.4$ argues for α-enrichment	Corr. at [Zn/Fe] $> +0.4$ argues for Fe depletion	
Cr/Fe vs. Zn/Fe	Anti-correlation	Suggests nucleosynthesis	Might be consistent with depletion	
Ti/Fe vs. Zn/Fe	No trend	Large Ti/Fe value at low Zn/Fe implies α-enrichment	Low Ti/Fe values at high Zn/Fe implies depletion	
Si/Ti vs. Zn/Fe	Correlation		Strong evidence for the depletion of Ti	
Si/Fe vs. [Si/H]	Plateau + Correlation	Plateau at [Si/H] < -1.5 argues for α-enrichment	Corr. at [Si/H] > -1 argues for Fe depletion	
Ni/Fe vs. [Si/H]	No trend			Mild enhancement difficult to account for
Si/Cr vs. [Si/H]	Correlation		Argues for depletion of Cr	
Si/Ni vs. [Si/H]	No trend		Contradicts Si/Fe, Si/Cr?	Photoionization?
S/Si vs. [Si/H]	No trend		Solar value implies no depletion	
Si/Al vs. [Fe/H]	No trend	Low Si/Al value contradicts halo stars		

consider several diagnostics for probing the likelihood and effects of dust obscuration.

5.1. *[X/H] vs.* N(HI)

Following the analysis of Boissé et al. (1998), we can examine metallicity trends with HI column density to search for evidence of dust obscuration. These authors identified an anti-correlation between [Zn/H] and N(HI) noting that the observed damped systems are constrained to have [Zn/H], N(HI) values in the following range: $19.8 <$ [Zn/H] $+ \log N(\mathrm{HI}) < 20.5$. The lower bound is simply the observational limit for detecting Zn, particularly in lower resolution observations (e.g. Pettini et al. 1994). Our database includes several upper limits and measurements below this lower threshold and the observed [Fe/H] values suggest many more systems. Boissé et al. interpreted the upper bound, meanwhile, as the result of dust obscuration, i.e., QAL surveys are biased against high metallicity, high N(HI) systems. We shall refer to this upper threshold as the 'obscuration threshold' for the remainder of the paper.

In Figure 21 we plot [X/H] values for three elements drawn from our database: (a) Zn, (b) Si, and (c) Fe. Overplotted as a dashed line in each panel is the obscuration threshold adopted by Boissé et al. (1998) with an offset of -0.4 dex for Fe to account for the observed enhancement of Zn/Fe. All of these elements generally follow the obscuration threshold, although one system (Q0458–02; the rightmost data point) probably exceeds the bound for Si. We stress that a strict obscuration threshold – as adopted by several authors – is both non-physical and apparently inconsistent with our observations. Instead, one should implement a more realistic treatment like the one introduced by Fall & Pei (1993) to accurately assess the effects of dust obscuration.

Although dust obscuration might explain the distribution of [X/H], N(HI) measurements presented in Figure 21, it does not *establish* that damped Lyα systems exhibit significant dust extinction. The absence of high [X/H], high N(HI) systems could very easily be explained by higher metallicity regions having significantly consumed HI gas and therefore lower HI column densities. In fact, one observes a mild anti-correlation between gas content and stellar metallicity in present-day spiral galaxies (Zaritsky, Kennicutt, & Huchra 1994). Therefore, systems with large N(HI) column densities might be more likely to reflect regions where star formation has yet to proceed in earnest. The absence might also reflect the detailed morphology of the damped Lyα systems. For example, the inner regions of protogalaxies might have HI 'holes' analogous to the holes observed in modern spiral galaxies including our own Galaxy (van Driel 1987; Wolfe & Prochaska 1998). Conversely, low N(HI) sightlines which show a range of metallicities, might probe both heavily enriched regions and the outer, less enriched regions of protogalaxies. To distinguish between these scenarios, one must consider more direct measures of dust extinction.

5.2. *Dust-to-gas ratio vs.* N(HI)

A more physically motivated approach for investigating dust obscuration than plotting [X/H] vs. N(HI) is to consider the trend of dust-to-gas ratios κ with HI column density. If dust obscuration is important, then large N(HI) systems should have lower dust-to-gas ratios independent of metallicity. We can calculate dust-to-gas ratios relative to the Galactic ISM by assuming the observed Zn/Fe enhancements are entirely due to dust depletion, i.e.,

$$\kappa^{Zn} \equiv (1 - 10^{-[\mathrm{Zn/Fe}]})\, 10^{[\mathrm{Zn/H}]} \quad . \tag{1}$$

Figure 22a presents κ^{Zn} values for the 19 systems exhibiting Zn in our full sample. Because [Zn/Si] ≈ 0 in these systems (the median [Si/Zn] value is $+0.03$), we can also consider the dust-to-gas ratios for Si,

$$\kappa^{Si} \equiv (1 - 10^{-[\mathrm{Si/Fe}]})\, 10^{[\mathrm{Si/H}]} \quad , \tag{2}$$

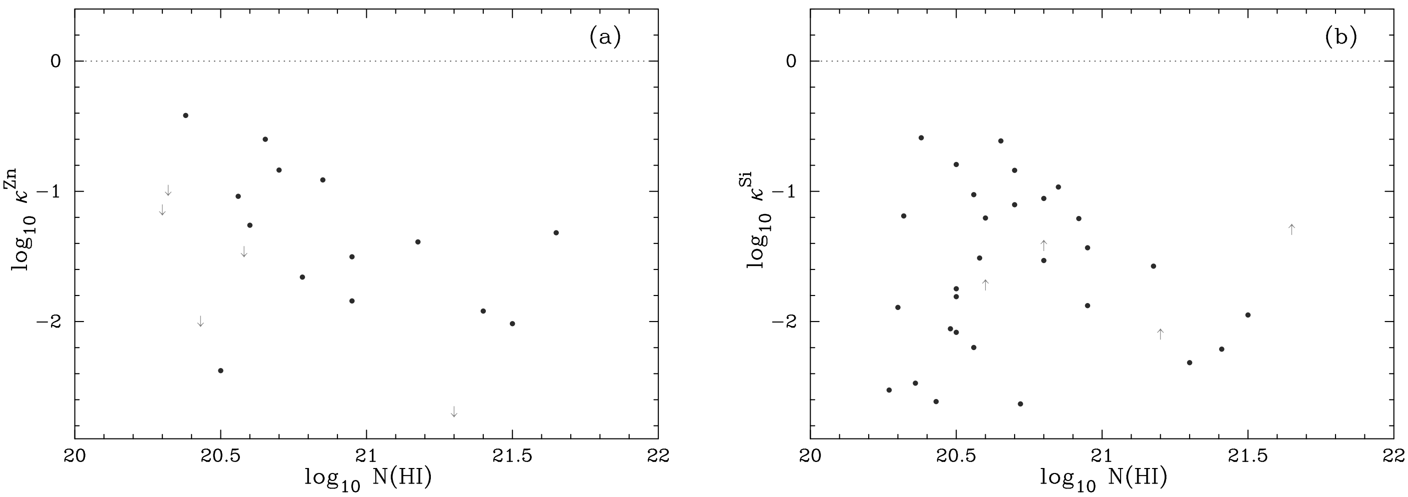

FIG. 22.— Plot of the dust-to-gas ratio κ vs. N(HI) inferred from the observed (a) Zn/Fe and (b) Si/Fe ratios. There is an absence of systems with large dust-to-gas ratios and large N(HI), which is consistent with – but not proof for – dust obscuration. In each case, the dotted line roughly corresponds to the dust-to-gas ratio of the ISM.

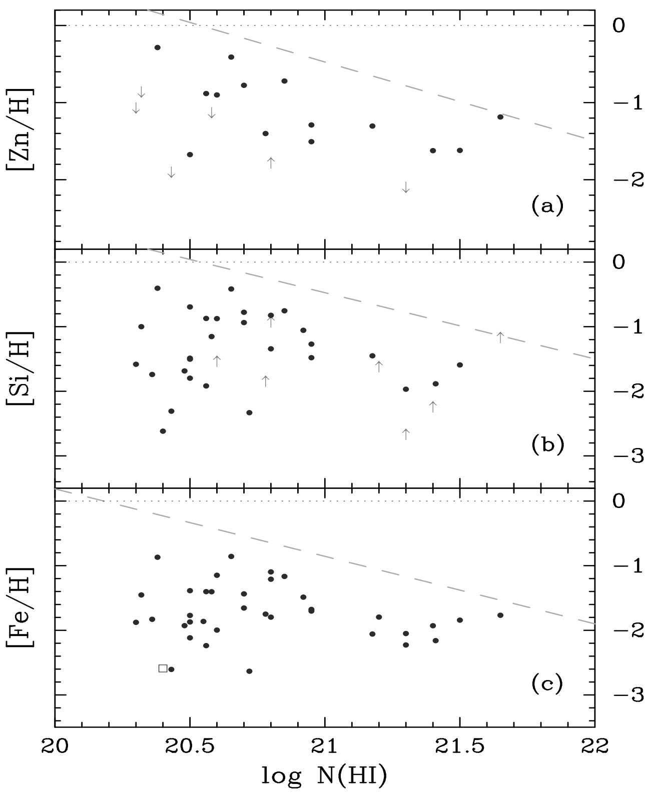

FIG. 21.— Plot of (a) [Zn/H], (b) [Si/H], and (c) [Fe/H] vs. N(HI). Boissé et al. (1998) and others have argued that the absence of measurements in the upper-right corner of each sub-panel is consistent with dust obscuration. While our observations support the trend identified by Boissé, we warn that they do not require the interpretation of dust obscuration.

which allows us to include many more systems (Figure 22b). We warn the reader, however, that a significant fraction of the observed Si/Fe (and Zn/Fe) enhancements might be the product of nucleosynthesis, not dust depletion. In this case, the values presented in Figure 22 must be considered *upper limits* to κ. In each sub-panel, the dotted line at $\log \kappa = 0$ roughly corresponds to the Milky Way dust-to-gas ratio where the majority of refractory elements are locked up in dust grains.

The damped Lyα dust-to-gas ratios follow the trends observed in Figure 21; the lower N(HI) sightlines exhibit a large range in κ while the higher N(HI) sightlines show only moderate to low values. The similarity between Figures 21 and 22 stems from the fact that the observed [Si/Fe] and [Zn/Fe] values are only mildly dependent on metallicity and N(HI). Like Figure 21, the observed distribution of κ, N(HI) pairs supports the notion that a sample of dusty, high N(HI) systems may be absent in our sample of damped Lyα systems.

5.3. *Implications for Extinction*

For dust obscuration to be important in damped Lyα surveys, the systems must contain enough dust to imply significant levels of dust extinction. Our approach is to combine the dust-to-gas ratios from the previous subsection with the known N(HI) values and an assumed extinction curve to estimate extinction corrections for a subset of our damped Lyα sample. To calculate the extinction $A(\lambda)$ at a given wavelength λ, we adopt an extinction curve $\xi(\lambda) \equiv A(\lambda)/A(V)$ and assume that

$$A(V) = 3.1 \cdot \frac{N(\mathrm{HI})}{5.9 \times 10^{21}\,\mathrm{cm}^{-2}} \cdot \kappa \qquad (3)$$

This is equivalent to assuming that $R_V \equiv A(V)/E(B-V) = 3.1$ and $N(\mathrm{HI}) = 5.9 \times 10^{21}\,\mathrm{cm}^{-2} E(B-V)$ (Bohlin et al. 1978). Inherent to this prescription is the presumption that the dust-to-gas ratio inferred from the depletion of Fe (i.e. κ^{Si}) corresponds to the dust-to-gas ratio of the dust responsible for extinction. Because the extinction in the FUV is dominated by small dust grains like silicates and iron oxides, the Fe depletion level should be a reasonably good tracer of the dust responsible for dust extinction in the damped Lyα systems. On the other hand, we again warn the reader that the probable nucleosynthetic contribution to the observed Si/Fe ratios implies the κ^{Si} values are strictly upper limits. We consider two extinction curves which hopefully bracket that for the damped Lyα systems: (1) MW – the Milky Way extinction law with $R_V = 3.1$ (Cardelli, Clayton, & Mathis 1989); and (2) SMC – the SMC extinction law (Prevot et al. 1984) with an extrapolation of the form $\xi(\lambda) \propto \lambda^{-1}$ at small λ. Finally, we limit the analysis to quasars discovered in surveys with reasonably well-defined filters X and limiting magnitudes m_{lim} (e.g. Wolfe et al. 1986; Storrie-Lombardi et al. 1996).

Figure 23 plots the extinction corrections $A(X)$ corresponding to the survey filter at the redshift of the damped Lyα system (e.g. 5400Å/[1+z_{abs}] for Wolfe et al. 1986) against the magnitude difference δ_m between the corrected magnitude of the quasar $m(X) - A(X)$ and the limiting magnitude of the survey m_{lim}. The shaded region denotes the parameter space where obscured objects lie, i.e. with unobscured magnitudes bright enough to satisfy the magnitude limit of the survey but with observed magnitudes obscured by the foreground damped Lyα system such that $m_X > m_{lim}$. Examining Figure 23, we find that the extinction values are small and that the $A(X), \delta_m$ pairs fill up only a small fraction of the allowed parameter space. Had the sample been significantly affected by obscuration, the distribution of points would be continuously distributed up to the shaded region and then cut off. With only one exception (the system toward Q0458–02), all of the $A(X) < 0.5$ mag. Even with the SMC dust curve, the range of $A(X)$ values is approximately 4× smaller than the spread in δ_m values. Qualitatively, at least, we expect that the distribution of obscured systems follows that of the observed distribution and therefore primarily occupies the cross-hatched region. Emboldened by the results presented in Figure 23, we draw two inferences from this exercise: (1) dust obscuration is biasing us against only a few damped Lyα systems; and (2) the absent systems have small $A(X)$ values, i.e. similar metallicity and dust depletion characteristics as our observed sample. It must be reemphasized that the dust-to-gas ratios we have adopted (κ^{Si}) assumes the Si/Fe enhancements have no nucleosynthetic contribution. We actually expect the systems are α-enhanced and, therefore, the κ^{Si} and $A(X)$ values should be considered upper limits which further strengthens our conclusions.

Finally, consider the extinction for a typical sightline through the Milky Way at low redshift. Assuming $\kappa \approx 1, N(\mathrm{HI}) = 10^{21}\,\mathrm{cm}^{-2}$, $R_V = 3.1$, and $\lambda_{abs} \approx 1250$Å, the implied extinction is 1.7 mag, i.e., more than twice the extinction of the damped Lyα system toward Q0458–02. Dust obscuration probably plays a far more significant role at $z < 1$ than high redshift, particularly given the small aperture afforded by HST for UV spectroscopy. Whether one must make corrections on the order of those implied by Pei & Fall (1995) remains to be seen, but it is obvious they must be considered. Maybe this explains, in part, the rarity of high luminosity optical counterparts for the few known low z damped Lyα systems (Turnshek et al. 2001). Hopefully, future studies will estimate extinction corrections and examine if they correlate with the optical counterparts.

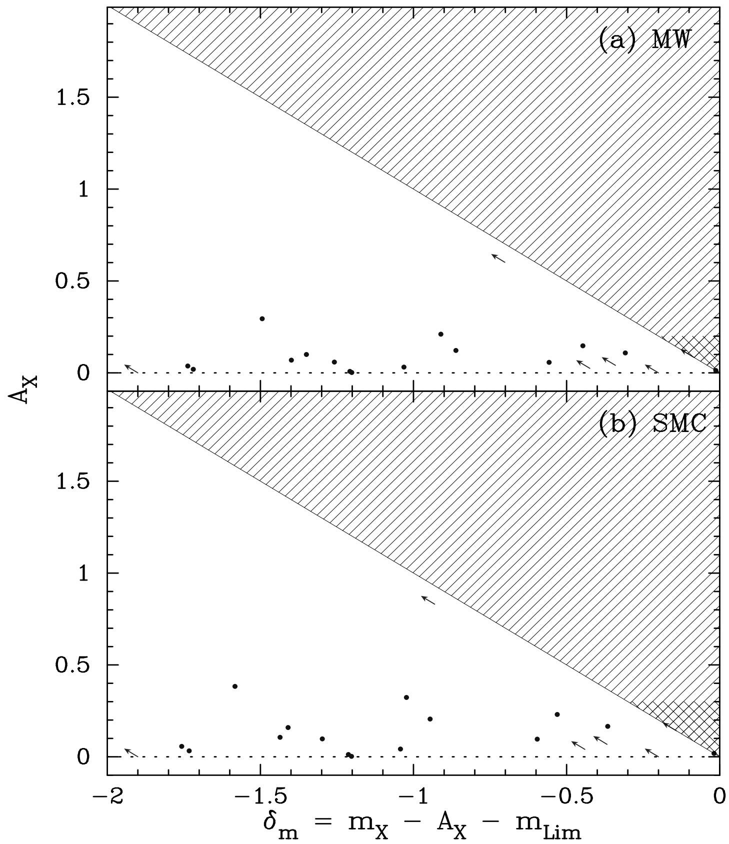

FIG. 23.— Extinction corrections $A(X)$ derived in the survey filter at the redshift of the foreground damped Lyα system against δ_m, the difference between the corrected brightness of the background quasar relative to the limiting magnitude of the damped Lyα survey. For the dust extinction curve, we consider two cases: (a) the Milky Way extinction law (Cardelli, Clayton, & Mathis 1989); and (b) the SMC law (Prevot et al. 1984). The shaded region denotes the area of parameter space which obscured quasars would occupy. In the several cases where the $N(\mathrm{Si}^+)$ values are lower limits, the values are plotted as diagonal arrows. Meanwhile, the cross-hatched region designates the area of parameter space which we contend is populated by damped Lyα obscured quasars as inferred by the observed distribution of $A(X), \delta_m$ values.

5.4. *[X/Zn] vs. [Zn/H]* + $\log N(\mathrm{HI})$ *Revisited*

In addition to implications for dust depletion, the results presented in Figure 17 (§ 3.2) offer insight about dust obscuration. As argued by Hou et al. (2001), the observed anti-correlations between [X/Zn] and N(Zn) are consistent with the effects of dust depletion with higher depletion levels at higher metal column densities. One would expect, however, the effects of dust obscuration to *minimize* the observed trend, i.e., systems with higher N(Zn) values ought to show higher [X/Zn] ratios (lower depletion

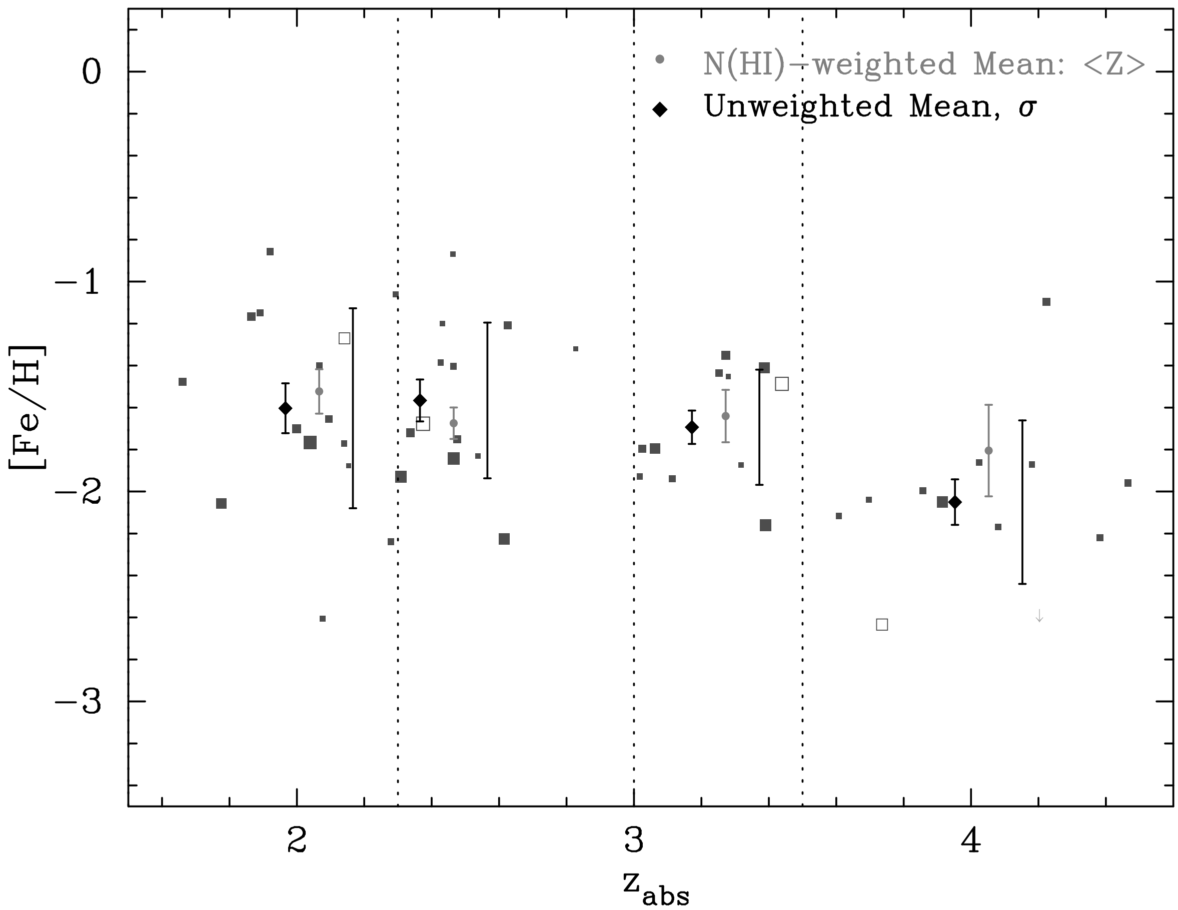

FIG. 24.— [Fe/H] vs. z_{abs} plot of the 50 damped Lyα systems which comprise the entire $z > 1.7$ sample. The open squares indicate systems where we consider a proxy for [Fe/H] (e.g. [Ni/H]). In all cases, the size of the data point is proportional to $\log N(\mathrm{HI})$. The dotted lines indicate 4 redshift intervals, arbitrarily chosen to evenly divide the systems. In each interval we plot three statistics: (1) the HI-weighted mean metallicity $< Z >$ represented by the solid circle with bootstrap error. It is plotted at the median redshift of each interval; (2) the unweighted mean logarithmic metallicity $<$ [Fe/H] $>$ with bootstrap error depicted by the solid diamond; and (3) the scatter in the individual systems σ([Fe/H]) represented by the vertical error bar.

levels) if dust obscuration were important. The general absence of such systems in Figure 17 is striking. Perhaps the processes of dust formation prohibit systems with low [Zn/X] when N(Zn) is large, but this seems contrived. We contend this serves as further evidence that dust obscuration is not strongly biasing the observed sample of damped systems.

6. CHEMICAL EVOLUTION

In previous papers we have investigated the chemical enrichment history of the universe in neutral gas through observations of the damped Lyα systems (PW99; PW00; PGW01). Although our current efforts focus on improving the statistics at $z_{abs} > 3$ with spectra obtained from the Echellette Spectrograph and Imager (ESI; Sheinis et al. 2001), the new HIRES sample significantly bolsters the measurements at high redshift. Figure 24 presents the [Fe/H] measurements from our complete sample including all of the systems presented in PGW01. Where we have adopted [Ni/H], [Al/H], or [Cr/H] as a proxy[6] for [Fe/H], we have plotted the value as an open square and have assumed an additional 0.1 dex error. In all cases, the size of the data point is linear with $\log N(\mathrm{HI})$. Following our previous analysis, we focus on three statistics of the [Fe/H], z_{abs} pairs: (i) the unweighted mean of the [Fe/H] values $<$ [Fe/H] $>$, (ii) the N(HI)-weighted mean $< Z >^{\mathrm{Fe}}$, and (iii) the rms dispersion σ([Fe/H]). Table 6 summarizes these statistics for four redshift intervals chosen to evenly split the sample as well as accommodate a natural division in the sample at $z_{abs} \approx 3$: $I_1 \rightarrow z_{abs} \,\epsilon\, (1.5, 2.3]$, $I_2 \rightarrow z_{abs} \,\epsilon\, (2.3, 3.0]$, $I_3 \rightarrow z_{abs} \,\epsilon\, (3.0, 3.5]$, and $I_4 \rightarrow z_{abs} \,\epsilon\, (3.5, 4.5]$. In Figure 24, the solid diamonds correspond to $<$ [Fe/H] $>$, the solid circles demarcate $< Z >^{\mathrm{Fe}}$ and are centered at the HI-weighted mean absorption redshift of each interval, and the unmarked error bars are σ([Fe/H]). For the mean statistics, the error on the points indicates the value from a bootstrap error anal-

[6]As discussed in § 2.1.1, we offset the [Ni/H], [Cr/H], and [Al/H] values by −0.1, −0.2, and 0.0 dex respectively.

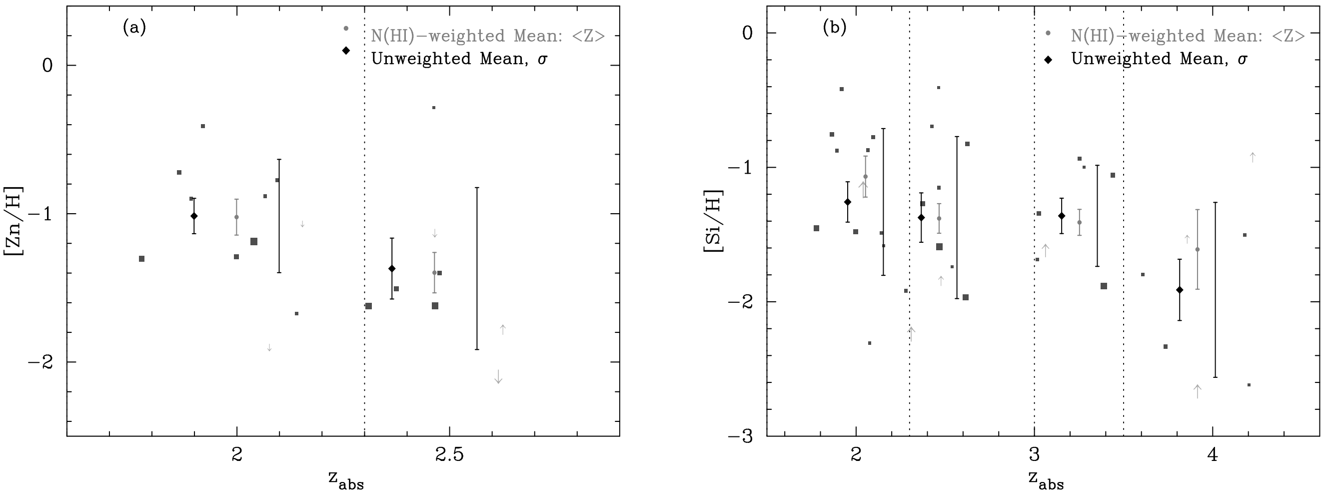

FIG. 25.— Similar to the previous figure except we have replaced Fe with (a) Zn and (b) Si, and we have restricted the analysis to our HIRES sample. In both cases, we have included limits in the statistical analysis with their measured value, a practice which has minimal impact on our conclusions.

ysis (e.g. PW00).

The results in Figure 24 are in good agreement with those presented in PGW01 but with an important difference. Previously, we noted a steady decrease in $<$ [Fe/H] $>$ with increasing redshift while $< Z >^{\rm Fe}$ remained nearly constant. The enlarged sample indicates a different picture: the $< Z >^{\rm Fe}$ and $<$ [Fe/H] $>$ statistics are in excellent agreement and exhibit very little evolution over the I_1, I_2 and I_3 intervals with the $<$ [Fe/H] $>$ statistic dropping sharply in I_4. Although the weighted mean remains nearly constant through all four intervals, the single system toward PSS1443+27 (the data point with [Fe/H] $\approx -1, z_{abs} \approx 4.2$) is heavily impacting both $< Z >^{\rm Fe}$ and σ([Fe/H]) in I_4. Eliminating it – a practice with no physical basis – would markedly revise these statistics because of its relatively large N(HI) and [Fe/H] values: $< Z >^{\rm Fe} = -2.07$, σ([Fe/H]) $= 0.26$ for I_4. In this case the $<$ [Fe/H] $>$ statistics would match the $< Z >^{\rm Fe}$ values at every epoch. Unless this is a coincidence, it suggests dust obscuration may not be significantly affecting the statistics.

With our HIRES observations, one can also examine the chemical evolution of the damped Lyα systems in elements other than the Fe-peak tracers. In the process, one can minimize the effects of dust depletion, but generally at the expense of introducing uncertainties associated with nucleosynthesis. In Figure 25 we plot (a) [Zn/H] and (b) [Si/H] vs. z_{abs} for our HIRES sample and Table 6 presents the same statistics that we measured for Fe. The results for Zn suggest a decline in $< Z >^{Zn}$ between the I_1 and I_2 intervals but our results are dominated by small number statistics. The larger sample presented by Pettini (1999) shows substantially less evolution. The results for Si, in contrast, are complicated by the significant number of lower limits on [Si/H]. For example, the sharp drop in $< Z >^{\rm Si}$ from I_1 to I_2 would be lessened if the lower limits in I_2 were resolved. Nevertheless, the [Si/H], z_{abs} values follow similar trends as those for [Fe/H]: a nearly constant unweighted mean from I_1 to I_3 followed by a sharp decline at $z_{abs} > 3.5$, a decreasing scatter (ignoring PSS1443+27), and a generally unevolving N(HI)-weighted mean. At present, there is more significant evolution in $< Z >^{\rm Si}$ than $< Z >^{\rm Fe}$ which we suggest is the result of small number statistics. We observe no evolution in [Si/Fe] with redshift (Figure 26) or any other quantity and therefore expect equal evolution in $< Z >^{\rm Si}$ and $< Z >^{\rm Fe}$ with complete statistics.

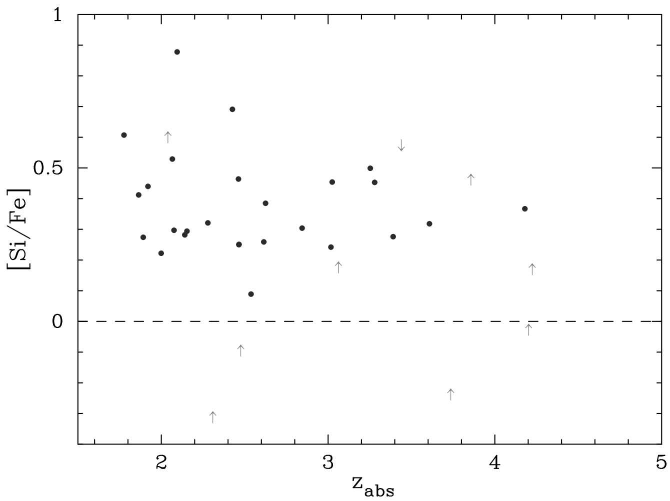

FIG. 26.— [Si/Fe] vs. z_{abs} for our complete sample. Although there is significant scatter, the [Si/Fe] enhancements remain nearly constant with redshift.

7. DISCUSSION AND SPECULATIONS

Each of the results described in the preceding sections has impact on an important area of damped Lyα chemical abundance research. Synthesizing these results, we

Table 6
CHEMICAL EVOLUTION

Elm	Stat	I_1	I_2	I_3	I_4
Fe					
	z_{min}	1.60	2.30	3.00	3.50
	z_{max}	2.30	3.00	3.50	4.50
	N	15	13	11	12
	z_{median}	2.07	2.47	3.27	4.05
	$<Z>^{Fe}$	-1.523 ± 0.106	-1.674 ± 0.075	-1.641 ± 0.125	-1.805 ± 0.218
	$<$ [Fe/H] $>$	-1.604 ± 0.119	-1.566 ± 0.100	-1.694 ± 0.079	-2.051 ± 0.108
	σ([Fe/H])	0.476	0.371	0.274	0.390
Si					
	z_{min}	1.60	2.30	3.00	3.50
	z_{max}	2.30	3.00	3.50	4.50
	N	12	10	7	7
	z_{median}	2.05	2.47	3.25	3.91
	$<Z>^{Si}$	-1.069 ± 0.152	-1.380 ± 0.110	-1.409 ± 0.097	-1.610 ± 0.296
	$<$ [Si/H] $>$	-1.258 ± 0.150	-1.374 ± 0.184	-1.361 ± 0.132	-1.911 ± 0.228
	σ([Si/H])	0.546	0.603	0.376	0.650
Zn					
	z_{min}	1.60	2.30		
	z_{max}	2.30	2.80		
	N	9	6		
	z_{median}	2.00	2.46		
	$<Z>^{Zn}$	-1.023 ± 0.121	-1.397 ± 0.136		
	$<$ [Zn/H] $>$	-1.016 ± 0.119	-1.370 ± 0.205		
	σ([Zn/H])	0.382	0.546		

find one characteristic stands out: the *uniformity* of the relative abundances of the damped Lyα systems. The observed abundance patterns – independent of the effects of nucleosynthetic enrichment, dust depletion, or photoionization – exhibit a remarkable similarity. Furthermore, the patterns are constant not only from system to system but also within a given damped Lyα system. In this section we discuss this homogeneity and its profound implications for the protogalactic population traced by the damped Lyα systems. We conclude with some speculations on the disparity between stellar and damped Lyα abundances and offer a list of immediate objectives for future research.

7.1. *Uniformity of the Observed Chemical Abundances*

With few exceptions, Figures 1–13 demonstrate minimal dependence of X/Fe on [Fe/H] metallicity. Aside from Si/Fe (and Si/Cr to lesser extent), the same conclusion holds if one considers Si/X against [Si/H]. Furthermore, there is no significant variation in the chemical abundances with redshift or HI column density. In short, the abundance patterns of the damped Lyα systems are strikingly similar. Of course, the relative abundances are not identical from system to system; there is a statistically significant dispersion in several of the abundance ratios. These departures from uniformity are likely explained by dust depletion.

By now, most of the community has concluded that the damped Lyα systems suffer from dust depletion. We have been more skeptical of this conclusion because the only evidence for dust depletion was the observed Zn/Fe enhancements and a tentative dust reddening result (Pei, Fall, & Bechtold 1991), the former of which is at least partially explained by nucleosynthesis. We are now convinced, however, that dust depletion explains the observed [Si/Fe] vs. [Zn/Fe] and [Si/Ti] vs. [Zn/Fe] correlations (Figures 14, 16) as well as the [X/Si] vs. N(Si) anti-correlations presented in Figure 18. Furthermore, the increase in [Si/Fe] at [Si/H] > -1 (Figure 19a) is naturally accommodated within a dust depletion scenario where higher metallicity gas has higher depletion levels. In turn, we expect that dust depletion explains most of the dispersion in the Zn/Fe and Si/Fe ratios and the small differences in the abundance patterns from system to system. Interestingly, the characteristics of depletion inferred from the observations also follow this theme of uniformity. First, the observed depletion levels are small (< 0.6 dex). Even in the extreme case that one interprets the Zn/Fe enhancements entirely in terms of depletion, the levels are far more representative of Galactic halo gas or the LMC than typical sightlines through our Galaxy. This presumably reflects the lower metallicity of the damped Lyα systems but may also correspond to lower density gas or physical processes which destroy dust grains[7]. The depletion levels implied by Zn/Fe or Si/Fe do not correlate with N(HI) or z_{abs} but only with metallicity at [Si/H] > -1. In fact, over 60% of the systems exhibit [Si/Fe] $= 0.3 \pm 0.1$ dex which we interpret as a floor imposed by nucleosynthesis. Finally, there is uniformity to the dust depletion levels within each damped system (PW96). With very few exceptions (notably the systems toward Q0347–38 and Q1759+75), the Si^+ profiles follow the Fe^+ profiles which track the Zn^+ profiles. On a velocity component by component basis, therefore, the depletion levels are constant throughout each system. As we argued in PW96, density fluctuations or regions shocked by supernovae ought to imply variations in the depletion levels. Instead, the damped Lyα systems tend

[7]We stress that dust obscuration would have very little impact on the observed depletion levels. The difference in dust-to-gas ratio between gas with [Zn/Fe] $= -0.5$ and [Zn/Fe] $= -1$ is nearly negligible (Equation 1).

to only show differences from galaxy to galaxy.

Because dust depletion modifies the gas-phase abundances of the damped Lyα systems, it complicates attempts to identify the underlying nucleosynthetic patterns. Presently, we feel dust corrections cannot be applied to the observed abundance ratios in a quantitative fashion. There are too many uncertainties associated with the composition of the dust grains, the processes of grain formation, and even identifying the base level of depletion. Regarding the latter point, previous authors have simply assumed the observed Zn/Fe enhancements are entirely the product of dust depletion, a presumption likely to be incorrect. Until significant advances are made in our understanding of the processes of dust depletion, introducing dust corrections will have limited value. Nevertheless, because the relative abundances show little variation with metallicity or any other property and the ratios with the largest dispersion (Zn/Fe, Si/Fe) are the most affected by dust depletion, this implies the nucleosynthetic patterns are very uniform. To assess the likelihood of nucleosynthetic variations, one can examine the Si/Fe ratios where offsets from the solar ratio could be expected from both nucleosynthesis and dust depletion (and even photoionization). Figure 7 indicates the observed scatter in [Si/Fe] is small: σ([Si/Fe]) = 0.14 dex. Because it is unlikely that dust depletion reduces the intrinsic scatter, the nucleosynthetic variation in Si/Fe from system to system is probably even smaller than the observed dispersion. This point is emphasized by the behavior of [Si/Fe] at [Si/H] < -1.5 dex (Figure 19a). At these metallicities, essentially every system exhibits [Si/Fe] $\approx +0.3$; the dispersion is less than 0.08 dex and is consistent with measurement error. The [Si/Fe] ratios indicate a very uniform enrichment history for the damped Lyα systems, i.e., proportionally similar enrichment from Type Ia and Type II SN. Allowing for the effects of dust depletion at [Si/H] > -1, this uniform enrichment history holds from [Si/H] $-2.5 \rightarrow -0.5$, a stunning range in metallicity. Furthermore, the odd-even effect, as probed by Si/Al, also shows no significant variation from system to system. Allowing for mild depletion in the damped Lyα systems, then, the nucleosynthetic patterns of the damped Lyα systems are essentially constant with metallicity, redshift, and N(HI).

The principal result of our examination of dust obscuration is that the majority of damped Lyα systems have very similar extinction properties; all but one system has an estimated extinction correction $A(X) < 0.5$ mag. Although this one outlier demonstrates that systems with significant extinction exist, the majority of the observed sample – and by inference we contend the majority of all damped Lyα systems – have minimal extinction. This implies that systems hidden from the damped Lyα surveys have similar characteristics to our observed sample, i.e., the observed uniformity in chemical abundances is not the result of dust obscuration.

Finally, we stress that the mean metallicity of the damped Lyα systems exhibits a temporal constancy. Both the unweighted and N(HI)-weighted mean metallicities demonstrate only mild evolution from $z = 1.5 \rightarrow 3.5$, an epoch spanning ≈ 2 Gyr where significant star formation is known to occur (Steidel et al. 1996). There appears to be a marked decline at $z > 3.5$, but by only the factor of a few. There may also be a decline in the dispersion of [Fe/H] values with increasing redshift, but this difference is also small. With the possible exception of the very highest redshift systems, therefore, the damped Lyα systems have an unevolving chemical enrichment history.

7.2. *Interpreting the Uniform Abundance Patterns*

The uniformity of the chemical abundances of the damped Lyα systems has profound implications for their enrichment history. It must be emphasized that the damped Lyα systems are *selected in absorption only according to their HI column density.* With the exception of dust obscuration – an issue we feel increasingly confident has minimal impact at high z – this selection criterion is unbiased. In turn, one expects the damped Lyα systems to correspond to the bulk of the protogalactic population, i.e., galaxies with a large range of mass, age, morphology, and chemical enrichment history. The actual distribution of protogalaxies is determined by the product of their number density and HI cross-sectional area (i.e. their optical depth, $\tau \equiv n\sigma_{HI}$). The observed chemical abundances, meanwhile, not only depend on the base properties of the galaxies, but also on gradients and variations within each galaxy. For example, sightlines will preferentially pass through the outer regions of galaxies with high central HI surface density simply because the available cross-section increases radially as r^2 but are restricted to the inner regions of systems with low central HI surface density. Therefore, one has every reason to expect large variations in the chemical abundances of the damped Lyα systems from system to system and within a given system.

In terms of the total metallicity of individual damped Lyα systems, a significant dispersion is observed (e.g. Figure 24). It is most pronounced at $z < 3$ which probably reflects protogalaxies with a greater range of mass and age than at $z > 3$. It is also more pronounced for sightlines with $N(\mathrm{HI}) < 10^{21}$ cm^{-2} which might indicate metallicity gradients within a given system. In terms of the relative abundances, however, the absence of significant variation is striking. At most, there are differences of ≈ 0.3 dex and these are almost entirely the product of dust depletion. This uniformity raises the following questions: Granted the dispersion in [Fe/H] and N(HI) values, why are the chemical abundance patterns and therefore the dust depletion and nucleosynthetic properties so similar? Furthermore, why do these properties exhibit such minimal evolution with redshift?

One possibility is that the damped Lyα systems are dominated by a subset of protogalaxies which have similar physical characteristics. Perhaps they arise in galaxies with the largest HI radial extent (e.g. Mo, Mao, & White 1998) or in a very large number of low mass galaxies. In this scenario, the range of N(HI) and [Fe/H] values would result from gradients within each galaxy. The systems would have similar enrichment histories and therefore possess similar nucleosynthetic patterns. It might be difficult to explain the constant mean metallicity with redshift, but perhaps this sub-population of galaxies has a small overall star formation rate. A more dramatic scenario to explain the relative abundance uniformity is that the nucleosynthetic histories of *all* protogalaxies at [Fe/H] < -1 are the same. The protogalactic abundance patterns we observe are derived from the convolution of the initial mass function (IMF) and the integrated star formation history. Although the concept of a universal IMF is widely supported, one might expect significant differences in the level and duration of star formation throughout the entire galactic population. In fact, it is these variations which presumably generate the differences in the observed abundances of various stellar populations. In order to explain the uniformity of the abundance patterns in this scenario, therefore, one may require a disparity between the damped Lyα and stellar abundances which we consider in the following sub-section.

While the constancy of the chemical abundances from system to system has important implications for the properties of high redshift protogalaxies, the uniformity within each system (as a function of velocity along the sightline) may place the tightest constraints on their physical nature. As first emphasized in PW96, the dominant ionic species (e.g. Fe^+, Si^+) show no significant variations from velocity component to component. This uniformity is not universal – the system toward GB1759+75 is an excellent counter-example (Prochaska, Howk, O'Meara, & Tytler 2002) – but holds for nearly every damped Lyα system in our sample. Therefore, there is little variation both in terms of dust depletion and nucleosynthesis at the presumably kpc scales resolved by the velocity profiles. If the observed variations in N(HI) and [Fe/H] are at least partly due to gradients in surface density and enrichment in these protogalaxies, then there must be very little radial variation in dust depletion or nucleosynthetic enrichment. Under the assumption that the absorption arises within a single protogalaxy, the observations indicate one or more of the following: (i) The mixing timescales are sufficiently small to yield constant relative abundances in these protogalaxies. For this to hold true, the timescale would have to be shorter than both the timescales for supernovae with significantly different yields (e.g. $\lesssim 1$ Gyr for Type Ia SN) and the timescale for dust grain formation; (ii) Abundance variations are washed out in velocity space because the observed velocity components are actually the superposition of many 'clouds', each with its own intrinsic abundances and dust depletion. Of course, it could be difficult to explain why the mean abundances of each component are so similar; (iii) The protogalactic volume probed by a damped Lyα observation is smaller than the scale where abundance differences are large. This scenario would require that the chemical filling-factor of protogalaxies to be very small at these epochs, an unlikely presumption. Furthermore, it would be very difficult to explain the kinematic characteristics observed from the low-ion profiles (Prochaska & Wolfe 1997b). Of these three possibilities, we believe efficient mixing is the most likely explanation.

On the other hand, if the damped Lyα profiles result from the superposition of absorption from several protogalaxies, then the observed uniformity places important constraints on the properties of the various 'clumps'. The most important result from our first study on damped Lyα velocity fields (Prochaska & Wolfe 1997b) is that protogalaxies as single disks within the CDM framework cannot reproduce our observations. This conclusion contradicted the protogalactic paradigm of the time (e.g. Kauffmann 1996; Mo, Mao, & White 1998) and inspired alternate protogalactic models within the CDM cosmology (Haehnelt et al. 1998; Maller et al. 2001). The key difference of the new scenarios is that the velocity profiles of the damped Lyα systems arise from the intersection with several protogalaxies. If these protogalactic clumps have formed independently, they should have unique metallicities, enrichment histories, and depletion levels. It may be very difficult to account for the chemical similarity among the low-ion profiles within this scenario. For the metal-poor systems (i.e. [Si/H] < -1.5), where we note little dispersion in any abundance ratio from sightline to sightline, the multiple clump scenario may not be challenged. The systems at [Si/H] > -1.5, in contrast, do exhibit variations in several ratios (e.g. Si/Fe and Zn/Cr) from system to system and might therefore be expected to show variations along the velocity profile. We emphasize that these systems tend to have larger velocity widths (Wolfe & Prochaska 1998), in fact these are the systems which *require* the multiple clump scenario within the CDM framework. At present, we cannot test the multiple clump scenario against our observations because these models provide at best crude predications for the dust properties and enrichment histories of the protogalactic clumps. We suspect, however, that these observations may ultimately pose a great challenge for theories of galaxy formation within the CDM cosmology.

7.3. *Gas-phase/Stellar Abundance Disparity*

The damped Lyα systems are the dominant neutral gas reservoirs of the universe. Therefore, it is natural to identify them as the fuel for past and present star formation and compare their abundance patterns with current stellar populations. An important property of the damped Lyα systems, however, is the fact that the majority have a very small molecular fraction (Petitjean et al. 2000). If the observed gas in the damped Lyα systems does fuel star formation, then there must be an intermediate stage which inspires the growth of molecular clouds. This suggests star formation is disconnected from the ISM of protogalaxies as probed by the damped Lyα systems. This disparity may manifest itself through contradictions in the abundance patterns of the damped Lyα systems with present-day stellar populations. For example, although we contend the damped Lyα systems exhibit α-enhancements similar to the Galactic halo stars, the damped Lyα Si/Al ratios are substantially lower than the observed stellar values. Furthermore, we have identified variations along the Fe-peak which may contradict the chemical abundance patterns of every stellar population.

Our observations might indicate that star formation occurs independent of the gas probed by our observations. This is not a profound supposition; star formation in the Milky Way is primarily restricted to dense molecular clouds whose filling factor is small. In this case, enrichment occurs independent of the global ISM and can proceed on very short timescales such that the stellar by-products have unique abundance patterns. We envision a scenario of star formation where the first stars to form in a molecular cloud should have abundances similar to the ISM, but star formation proceeds rapidly through several generations with the subsequent stellar populations more closely reflecting the rapidly changing abundances of the molecular cloud. Although supernovae feedback will ultimately distribute the metals of the molecular cloud to the ambient ISM, the effects on the mean abundances might be small. This would be particularly true if the majority of metals are carried out to the local IGM instead (e.g. Mac Low & Ferrara 1999; Kubulnicky & Skillman 1997). In short, one can envision an ISM mildly enriched by the byproducts of molecular clouds, each with its own metallicity and relative chemical abundances giving mean abundances different from observed stellar populations.

Star formation may also have significant impact on the protogalactic population selected by damped Lyα systems. There are two competing processes affecting the damped Lyα cross-section of a given galaxy. As galaxies form through the accretion and dissipation of gas, their HI surface densities will increase until they have an appreciable surface density with $N(\mathrm{HI}) > 2 \times 10^{20}\,\mathrm{cm}^{-2}$. On the other hand, star formation lowers the surface density through the consumption of gas and the feedback from supernovae. Qualitatively, we expect the damped Lyα systems to more frequently probe galaxies in the early stages of formation, in particular prior to significant star formation. This might well explain the lack of chemical evolution observed in the damped systems: at every epoch the damped Lyα systems are predominantly gas-rich, metal-poor galaxies. Systems which have experienced bursts of star formation (e.g. the Lyman break galaxies) may have consumed or blown out an appreciable fraction of their HI gas and have a comparatively small damped Lyα cross-section.

7.4. *Future Directions/Objectives*

In closing, we present an abundance wish list for the damped Lyα systems. Achieving these goals will markedly improve our understanding of the chemical abundances of the damped Lyα systems. We expect most, if not all, will be accomplished in the next five years through the active efforts of our group and others throughout the community.

1. A comparison of the relative abundance of the α-elements (Si, S, O, Ar, Ti) in several damped Lyα systems. In this paper, we have already demonstrated the importance of Si/Ti and S/Si for considerations of dust depletion. Comparisons among the α-elements will provide further insight into photoionization, nucleosynthesis, and dust depletion.

2. Measurements of Mn at $z_{abs} > 1.5$. We must ascertain if Mn/Fe is universally sub-solar in the damped Lyα systems.

3. Relative abundance measurements for a sample of $z_{abs} < 1$ damped systems at $\lambda_{rest} < 1500$Å. Although this will require space-based observations, these measurements are critical to unveiling the evolution of galactic chemical abundances.

4. An investigation of the odd-even effect at all metallicities. This will require a number of P II measurements in the more metal-rich systems.

5. Empirical evidence for/against photoionization. With the advent of UV-sensitive ($\lambda < 4000$Å) echelle spectrographs, one should be able to examine ions like Fe III and C III to constrain the effects of photoionization.

6. Over 100 damped Lyα metallicity measurements. These observations are still the most efficient means for testing chemical evolution scenarios at any epoch.

7. A survey of radio-selected quasars for damped Lyα systems. This is the ideal approach for assessing the impact of dust obscuration on the damped Lyα surveys. Ellison et al. (2001) have been pursuing such a program and the first results are forthcoming.

8. Better oscillator strengths for a number of transitions including Fe II 1611.

9. A measurement of at least one element with Z$>$ 30. This will require a very special damped Lyα system, i.e., one with very high HI column density and metallicity in front of a very bright quasar.

10. Additional emphasis on the systems with [Si/Fe] $> +0.4$ dex to better evaluate the dust characteristics of the damped Lyα systems.

The authors wish to extend special thanks to those of Hawaiian ancestry on whose sacred mountain we are privileged to be guests. Without their generous hospitality, none of the observations presented herein would have been possible. We thank Chris Howk, Max Pettini, and Eric Gawiser for stimulating discussions and very helpful comments. J.X.P. acknowledges support from a Carnegie postdoctoral fellowship. AMW was partially supported by NSF grant AST 0071257.

APPENDIX

DUST CORRECTIONS

In this section we examine the implications of the dust correction formalism introduced by Vladilo (1998). The principle premise of his treatment is that dust in the damped Lyα systems has the same average number of atoms of each element per grain as Galactic dust. As we show below, this has the effect of minimizing departures from solar relative abundance for our observed abundance ratios.

Let us represent the number of atoms of Fe in the gas and dust phases as n_g^{Fe} and n_d^{Fe} respectively. For a system that is 90% depleted, this implies the dust fraction $\xi(\mathrm{Fe}) \equiv n_d^{Fe}/(n_d^{Fe} + n_g^{Fe}) = 0.9$. Now consider the abundances of an element X with a dust fraction $\xi(\mathrm{X}) \equiv n_d^X/(n_d^X + n_g^X)$. Assume that in the Galactic ISM element X depletes relative to Fe like

$$\theta^X = \frac{n_d^X}{n_d^{Fe}} \quad . \tag{A1}$$

The prescription introduced by (Vladilo 1998) is to assume that this ratio applies to the damped Lyα systems *independent of the intrinsic abundances of the system.* This has important implications for the depletion of element X relative to Fe in the damped Lyα systems as inferred from their gas-phase abundances. Consider the relative dust fraction of element X to Fe:

$$D^X \equiv \frac{\xi(\mathrm{X})}{\xi(\mathrm{Fe})} \tag{A2}$$

$$= \frac{n_d^X}{n_d^X + n_g^X} \cdot \frac{n_d^{Fe}}{n_d^{Fe} + n_g^{Fe}} \tag{A3}$$

$$= \frac{\theta^X n_d^{Fe}}{\theta^X n_d^{Fe} + n_g^X} \cdot \frac{n_d^{Fe}}{n_d^{Fe} + n_g^{Fe}} \tag{A4}$$

$$= \frac{1 + \frac{n_d^{Fe}}{n_g^{Fe}}}{\frac{n_g^X}{\theta^X n_g^{Fe}} + \frac{n_d^{Fe}}{n_g^{Fe}}} \tag{A5}$$

The last expression demonstrates that $D^X > 1$ if $n_g^X / n_g^{Fe} < \theta^X$, i.e. if the observed gas-phase ratio of X/Fe is less than the dust composition in the Galactic ISM. Therefore, elements with low [X/Fe] values will tend to have larger dust corrections which serve to minimize any departure of X/Fe from the solar abundances. Conversely, $D^X < 1$ if the observed ratio of X/Fe is greater than the dust ratio in the ISM.

It is best to illustrate this effect with an example. In the ISM, Mn has a similar refractory nature as Fe: $\xi(\mathrm{Mn})_{ISM} = \xi(\mathrm{Fe})_{ISM}$. This implies that

$$\theta^{Mn} = \frac{n_d^{Mn}}{n_d^{Fe}} \approx \frac{10^{\epsilon(\mathrm{Mn})}}{10^{\epsilon(\mathrm{Fe})}} \approx \frac{1}{100} \tag{A6}$$

where ϵ(Mn) and ϵ(Fe) are the solar abundances of Mn and Fe. In the damped Lyα systems, one observes $n_g^{Mn}/n_g^{Fe} \approx 1/200$ and therefore $D^{Mn} > 1$ implying a higher fraction of Mn is in the dust phase than Fe. Therefore, when one applies a dust correction to the observed Mn/Fe ratio, the resulting value is closer to the solar ratio of $\approx 1/100$. A similar effect holds for a mildly refractory element like Si. Because the Si/Fe ratio observed in the damped systems is much larger than θ^{Si} from the ISM, the dust correction to Si is much smaller than for Fe and the observed Si/Fe is corrected downward to the solar value when dust corrections are applied.

In short, the prescription introduced by Vladilo (1998), which makes an nonphysical assumption about the formation of dust grains, tends to minimize observed departures from solar for all of the X/Fe ratios.

REFERENCES

Arnett, W.D. 1971, ApJ166, 153
Bergeson, S.D., Mullman, K.L., Wickliffe, M.W., Lawler, J.E., Litzen, U., and Johansson, S. 1996, ApJ464, 1044
Bohlin, R.C., Savage, B.D., & Drake, J.F. 1978, ApJ, 224, 132
Boissé, P., Le Brun, V., Bergeron, J., & Deharveng, J.-M. 1998, A&A, 333, 841
Cardelli, J.A., Clayton, G.C., & Mathis, J.S. 1989, ApJ, 345, 245
Cardelli, J.A., Savage, B.D., & Ebbets, D.C. 1991, ApJ, 452, L275
Cardelli, J.A. and Savage, B.D. 1995, ApJ, 452, 275
Carretta, E., Gratton, R. G., & Sneden, C. 2000, A&A, 356, 238
Edvardsson, B., Anderson, J., Gutasfsson, B., Lambert, D.L., Nissen, P.E., and Tompkin, J. 1993, A&A, 275, 101.
Ellison, S.L., Ryan, S., & Prochaska, J.X. 2001 MNRAS, 326, 628
Ellison, S.L., Yan, L., Hook, I.M., Pettini, M., Wall, J.V., & Shaver, P. 2001, A&A, in press (astro-ph/0109205)
Fall, S.M. & Pei, Y.C. 1993, ApJ, 402, 479
Grevesse, N., Noels, A., & Sauval, A.J. 1996, In: Cosmic Abundances, S. Holt and G. Sonneborn (eds.), ASPCS, V. 99, (BookCrafters: San Fransisco), p. 117
Haehnelt, M.G., Steinmetz, M. & Rauch, M. 1998, ApJ, 495, 647
Heger & Woosley, S. 2001, ApJ, submitted (astro-ph/0110015)
Henry, R.B.C. & Worthey, G. 1999, PASP, 111, 919
Hoffman, R.D. et al. 1996, ApJ, 460, 478
Hou, J.L., Boissier, S., & Prantzos, N. 2001, A&A, 370, 23
Howk, J.C. & Savage, B.D. 1999, ApJ, 517, 746
Howk, J.C. & Sembach, K.R. 1999, ApJ, 523, 141L
Howk, J.C., Savage, B.D., & Fabian, D. 1999, ApJ, 525, 253
Jenkins, E.B. 1987, in Interstellar Processes ed. D.J. Hollenbach and H.A. Thronson, Jr. (Boston: D. Reidel Publishing Company), p. 533
Johnson, J.A. 2001, AJ, submitted
Kauffmann, G. 1996, MNRAS, 281, 475
Kubulnicky, H.A. & Skillman, E. 1997, ApJ, 489, 636
Kulkarni, V.P., Fall, S.M., & Truran, J.W. 1997, ApJ, 484, 7
Lanzetta, K. M., Wolfe, A. M.,& Turnshek 1995, ApJ, 440, 435
Lu, L., Sargent, W.L.W., Barlow, T.A., Churchill, C.W., & Vogt, S. 1996, ApJS, 107, 475
Lu, L., Sargent, W.L.W., & Barlow, T.A. 1999, in Highly Redshifted Radio Lines ed. C.L. Carilli, S.J.E. Radford, K.M. Menten, and G.I. Langston (San Fransisco: BookCrafters Inc.), p.132 (astro-ph/9711298)
Mac Low, M.-M. & Ferrara, A. 1999, ApJ, 513, 142
Maller, A.H., Prochaska, J.X., Somerville, R.S., & Primack, J.R. 2001, MNRAS, 326, 1475
McWilliam, A., Preston, G.W., Sneden, C., & Searle,L. 1995, AJ, 109, 2757
McWilliam, A. 1997, ARA&A, 35, 503
Meyer, B.S., Krishnan, T.D., & Clayton, D.D. 1996, ApJ, 462, 825
Mo, H.J., Mao, S., & White, S.D.M. 1998, MNRAS, 295, 319
Molaro, P., Bonifacio, P., Centurión, M., D'Odorico, S., Vladilo, G., Santin, P., & Di Marcantonio, P. 2000, ApJ, 541, 54
Molaro, P., Levshakov, S.A., D'Odorico, S., Bonifacio, P., & Centuríon, M. 2001, ApJ, 549, 90
Ostriker, J.P. & Heisler, J. 1984, ApJ, 278, 1
Outram, P.J., Chaffee, F.H., & Carswell, R.F. 1999, MNRAS, 310, 289
Pei, Y.C., Fall, S.M., & Bechtold, J. 1991, ApJ378, 6
Pei, Y.C. & Fall, S.M. 1995, ApJ, 454, 69
Petitjean, P., Srianand, R., & Ledoux, C. 2000, A&A, 364, 26L
Pettini, M., Smith, L. J., Hunstead, R. W., and King, D. L. 1994, ApJ, 426, 79
Pettini, M., Smith, L.J., King, D.L., & Hunstead, R.W. 1997, ApJ, 486, 665
Pettini, M., Ellison, S.L., Steidel, C.C., & Bowen, D.V. 1999, ApJ, 510, 576
Pettini, M. 1999, in Lecture Notes in Physics, Proceedings of ESO Workshop, ed. J. Walsh and M. Rosa (Berlin: Springer), in press, astro-ph/9902173
Prevot, M.L., Lequeux, J., Maurice, E., Prevot, L., & Rocca-Volmerange, B. 1984, Astr. Ap., 132, 389
Primas,F., Reimers, D., Wisotzki, L., Reetz, J., Gehren, T., & Beers, T.C. 2000, in The First Stars, ed. A. Weiss, T. Abel, & V. Hill (Berlin: Springer), 51
Prochaska, J.X. 1999, ApJ, 511, L71
Prochaska, J. X. & Wolfe, A. M. 1996, ApJ, 470, 403 (PW96)
Prochaska, J. X. & Wolfe, A. M. 1997, ApJ, 474, 140
Prochaska, J. X. & Wolfe, A. M. 1997, ApJ, 486, 73
Prochaska, J. X. & Wolfe, A. M. 1999, ApJS, 121, 369 (PW99)
Prochaska, J.X. & Wolfe, A.M., 2000, ApJ, 533, L5 (PW00)
Prochaska, J. X., Naumov, S.O., Carney, B.W., McWilliam, A., & Wolfe, A.M. 2000, AJ, 120, 2513 (P00)
Prochaska, J.X., Gawiser, E., & Wolfe, A.M. 2001, ApJ, 552, 99
Prochaska, J.X., Wolfe, A.M., Tytler, D., Burles, S.M., Cooke, J., Gawiser, E., Kirkman, D., O'Meara, J.M., & Storrie-Lombardi, L. 2001, ApJS, in press
Prochaska, J.X. & Wolfe, A.M. 2001, in prep
Prochaska, J.X., Howk, J.C., O'Meara, J.M., & Tytler, D. 2001, ApJ, in prep
Raassen, A.J.J. & Uylings, P.H.M. 1998, A&A, 340, 300
Richards, E.A. 1999, ApJ, 513, 9L
Savage, B. D. and Sembach, K. R. 1991, ApJ, 379, 245
Savage, B.D., Cardelli, J.A., & Sofia, U.J. 1992, ApJ, 401, 706
Savage, B. D. & Sembach, K. R. 1996, ARA&A, 34, 279
Sembach, K.R., Steidel, C.C., Macke, R.J., and Meyer, D.M. 1995, ApJ, 445, L27
Sheinis, A.I., Miller, J., Bigelow, B., Bolte, M., Epps, H., Kibrick, R., Radovan, M., & Sutin, B. 2001, PASP, submitted
Smecker-Hane, T. & McWilliam, A. 2001, in preparation

Sneden, C., Gratton, R.G., & Crocker, D.A. 1991, A & A, 246, 354
Sofia, U.J. & Jenkins, E.B. 1998, ApJ, 499, 951
Spitzer, L., & Fitzpatrick, E.L. 1993, ApJ, 409, 299
Steidel, C.C., Giavalisco, M., Dickinson, M., & Adelberger, K.L. 1996, ApJ, 112, 352
Steidel, C.C., Adelberger, K., Dickinson, M., Giavalisco, M., Pettini, M., & Kellogg, M. 1998, ApJ, 492, 428
Storrie-Lombardi, L.J., Irwin, M.J. 1996, & McMahon, R.G. MNRAS, 282, 1330
Storrie-Lombardi, L.J. & Wolfe, A.M. 2000, ApJ, 543, 552
Timmes, F.X., Woosley, S.E. & Weaver, T.A. 1995, ApJS, 98, 617
Turnshek, D.A., Rao, S., Nestor, D., Lane, W., Monier, E., Bergeron, J., & Smette, A. 2001, in *Gas and Galaxy Evolution*, ASP Conf. Series, eds. Hibbard, Rupen, & van Gorkum
Umeda, H. & Nomoto, K. 2001, ApJ, in press (astro-ph/0103241)
van Driel, Willem 1987, University of Gronigen, PhD thesis
Viegas, S.M. 1994, MNRAS, 276, 268
Vladilo, G. 1998, ApJ, 493, 583
Vladilo, G., Centurión, M., Bonifacio, P., & Howk, J.C. 2001, ApJ, 557, 1007
Vogt, S.S., Allen, S.L., Bigelow, B.C., Bresee, L., Brown, B., et al. 1994, SPIE, 2198, 362
Wakker, B.P. & Mathis, J.S. 2000, ApJ, 554, L107
Wallerstein, G., et al. 1997, Rev. Mod. Phys. 69, 995
Welty, D.E., Lauroesch, J.T., Blades, J.C., Hobbs, L.M., & York, D.G. 1997, ApJ, 489, 672
Wheeler, J.C., Sneden, C., & Truran, J.W.Jr. 1989, ARA & A, 27, 279
Wiese, L.M., Fedchak, J. A., & Lawler, J. E. 2001, ApJ, 547, 1178
Wolfe, A.M., Turnshek, D.A., Smith, H.E., & Cohen, R.D. 1986, ApJS, 61, 249
Wolfe, A. M., Fan, X-M., Tytler, D., Vogt, S. S., Keane, M. J., & and Lanzetta, K. M. 1994, ApJ, 435, L101
Wolfe, A. M., Lanzetta, K. M., Foltz, C. B., and Chaffee, F. H. 1995, ApJ, 454, 698
Wolfe, A.M. & Prochaska, J.X. 1998, ApJ, 494, 15L
Wolfe, A.M., Prochaska, J.X., & Gawiser, E. 2001, in preparation
Wolfe, A. M. & Prochaska, J.X. 2000a, ApJ, 545, 591
Woosley, S.E. & Weaver, T.A. 1995, ApJS, 101, 181
Zaritsky, D., Kennicutt, R.C.,Jr., & Huchra, J.P. 1994, ApJ, 420, 87
Zsargó, J. & Federman, S.R. 1998, ApJ, 498, 256